Published in final edited form as:
Autoimmunity. 2013 May ; 46(3): 188–204. doi:10.3109/08916934.2012.746671.

Regulation of basement membrane-reactive B cells in BXSB, (NZBxNZW)F1, NZB, and MRL/lpr lupus mice

Amy G. Clark[*], **Qihua Fan**[*], **Graham F. Brady**[*], **Katherine M. Mackin**[*], **Evan D. Coffman**[*], **Melissa L. Weston**[*], and **Mary H. Foster**[*]

[*]Department of Medicine, Duke University Medical Center, Box 103015, Durham, NC, 27710, and Research Service, Durham VAMC, Durham, NC, 27705, USA

Abstract

Autoantibodies to diverse antigens escape regulation in systemic lupus erythematosus under the influence of a multitude of predisposing genes. To gain insight into the differential impact of diverse genetic backgrounds on tolerance mechanisms controlling autoantibody production in lupus, we established a single lupus-derived nephritis associated anti-basement membrane Ig transgene on each of four inbred murine lupus strains, including BXSB, (NZBxNZW)F1, NZB, and MRL/lpr, as approved by the Duke University and the Durham Veterans Affairs Medical Centers' Animal Care and Use Committees. In nonautoimmune C57BL/6 mice, B cells bearing this anti-laminin Ig transgene are stringently regulated by central deletion, editing, and anergy. Here, we show that tolerance is generally intact in unmanipulated Ig transgenic BXSB, (NZBxNZW)F1, and NZB mice, based on absence of serum transgenic anti-laminin autoantibodies and failure to recover spontaneous anti-laminin monoclonal antibodies. Four- to six-fold depletion of splenic B cells in transgenic mice of these strains, as well as in MRL/lpr transgenic mice, and reduced frequency of IgM+ bone marrow B cells suggest that central deletion is grossly intact. Nonetheless the four strains demonstrate distinct transgenic B cell phenotypes, including endotoxin-stimulated production of anti-laminin antibodies by B cells from transgenic NZB mice, and in vitro hyperproliferation of both endotoxin- and BCR-stimulated B cells from transgenic BXSB mice, which are shown to have an enrichment of CD21-high marginal zone cells. Rare anti-laminin transgenic B cells spontaneously escape tolerance in MRL/lpr mice. Further study of the mechanisms underlying these strain-specific B cell fates will provide insight into genetic modification of humoral autoimmunity in lupus.

Keywords

autoantibodies; tolerance; transgenic mice; deletion; laminin

Introduction

Systemic lupus erythematosus (SLE) is a debilitating autoimmune disease with diverse clinical manifestations. Glomerulonephritis is one of the most severe manifestations of SLE, affecting up to 74% of patients and often leading to dialysis or transplantation. Yet pathogenic mechanisms remain poorly understood. Newer immunosuppressive agents and biologics (anti-CD20, anti-BLyS) have only recently begun to replace cyclophosphamide as therapy, and relapses and serious side effects continue to plague patients. New disease- and

Address Correspondence: Mary H. Foster, Nephrology Research, Duke University Medical Center, Box 103015, Durham, NC 27710, Phone 1-919-684-9788, FAX 1-919-684-3011, mhfoster@dm.duke.edu.

mechanism-based interventions are urgently needed, but their rational design will require better understanding of disease pathogenesis.

The autoantibodies and autoreactive T cells that contribute to kidney and other organ damage in SLE arise as a result of failed tolerance, the fundamental immunologic abnormality in lupus. Insights into the basis of tolerance defects are emerging from the complementary study of human and murine lupus, although rapid progress has been hindered by the genetic complexity and clinical and serological heterogeneity of this disease. Genome-wide association studies have already identified approximately 40 lupus susceptibility loci in man [1, 2], and a similar number of murine susceptibility loci have been validated to date in congenic mice [3–5]. Of the individual genes established as risk factors to date, many are involved in B and/or T cell signaling or survival [4, 6–11]. Assigning functions to genetic variants and mechanistic dissection has been slowed, however, by reliance on lupus as a single phenotype in many studies, inconsistent phenotype penetrance due to varied environmental exposures, or by tracking broad phenotypes such as mortality, anti-DNA Ig production, or nephritis, that are polygenic in origin or absent in a significant proportion of patients (e.g., anti-dsDNA Ig are found in only ~50% of patients) [12].

It is in this context that we began a systematic approach to study failed tolerance in murine lupus nephritis. We and others [13] have reasoned that the genetic complexity of lupus in the outbred human population may be best modeled by integrated study of the major inbred lupus strains, each of which has a unique constellation of lupus susceptibility genes. We also reasoned that the influence of a given genetic background could be measured using tractable, quantifiable tolerance phenotypes, such that deviations from normal phenotype can be quantified and characterized, and ultimately analyzed for underlying mechanisms and linked to genetic background and eventually to specific genes. For this purpose, we modified New Zealand Black (NZB/BINJ, or NZB), NZBWF1/J [(NZBxNZW)F1, or BWF1], BXSB/MpJ (BXSB), and MRL/MpJ-Fas^{lpr}/J (MRL/lpr) mice to express the identical lupus nephritis-associated anti-laminin LamH Ig transgene (Tg), using at least 9 generation backcrosses. We chose three classic lupus strains, BXSB, BWF1, and MRL/lpr, because each develops accelerated nephritis, suggesting early and rapid loss of tolerance in nephritogenic clones. The fourth lupus strain, NZB, develops kidney disease late in life but carries multiple major susceptibility loci that contribute to severe nephritis in strains BWF1, (SWRxNZB)F1 (SNF1), and NZM2410 [4].

The LamH Ig Tg was particularly suited for this purpose. It is derived from an MRL/lpr lupus mAb and binds a kidney basement membrane antigen implicated in both mouse and human SLE [14–19]. A pathogenic role is suggested by the ability of epitope-bearing laminin peptides to suppress MRL/lpr lupus nephritis [17]. The LamH Tg encodes a dominant Ig heavy chain capable of forming anti-laminin Ig when paired with a wide variety of endogenous light chains [20]. B cells from multiple LamH Ig Tg lines are stringently regulated in the non-autoimmune C57BL/6 (B6) strain by a combination of central deletion, editing, and anergy, such that Tg-encoded anti-laminin antibodies are rarely detected in sera, either spontaneously or after mouse exposure to endotoxin or antigen in adjuvant [21, 22]. Compared to their non-Tg B6 littermates, Tg B6 mice have 8-9-fold fewer spleen B cells (mean 6 million total), a number that drops to a mere 1.2 million in LamH/Vk8Jk5 H+LL Ig Tg mice in which kappa light chain editing is prevented by homozygosity at the targeted kappa allele [21, 22]. Residual B6 Tg spleen B cells are shortlived and fail to secrete anti-laminin Ig after endotoxin stimulation. This cell phenotype is preserved in the MRL/MpJ strain [21], although notably microarray analyses reveal strain differences in anergic B cell gene expression [23]. Thus, the LamH Ig Tg model provides a stable, well defined tolerance

phenotype useful for the study of autoreactive B cell fates in the context of aggressive SLE models.

Herein we report the fate of LamH Ig Tg cells in each of the four lupus strains, measuring parameters previously used to analyze their fate in the B6 strain. We find that whereas central deletion of a prominent subset of Tg B cells and peripheral tolerance checkpoints appear grossly intact, each strain nonetheless demonstrates a unique Tg B cell phenotype, distinct from each other and from the tolerance phenotype observed in non-autoimmune B6 Tg mice. In contrast to results in other strains, anti-laminin Tg Ig are readily recovered from LPS-stimulated spleen B cells, and can be induced in vivo in a subset, of NZB Tg mice. BXSB Tg B cells uniquely upregulate CD21 with an enhanced CD1d+ marginal zone B cell subset, express high density surface Tg receptors, and hyperproliferate to both B cell receptor crosslinking and LPS. Occasional Tg anti-laminin B cells are spontaneously activated in vivo in a subset of MRL/lpr Tg mice, whereas the fate of Tg B cells in BWF1 Tg mice most closely resembles the tolerance phenotype observed in the non-autoimmune B6 strain. Thus strain-dependent lupus susceptibility differentially modifies Tg B cell fate and tolerance. Dissection of the molecular basis of these differences will provide further insight into the complex genetics of lupus and hopefully assist in identifying additional patient-specific therapeutic targets

Materials & Methods

Animals

Generation of the anti-laminin LamH IgM heavy chain construct and characterization of LamH Ig transgenic (Tg+) mice on both the non-autoimmune B6 and the autoimmune MRL/MpJ (MRL) backgrounds were described previously [21, 22, 24]. Hemizygous Tg+ and non-transgenic mice were reared under conventional specific pathogen-free conditions in the vivarium of the Durham Veterans Affairs Medical Center. All Tg+ mice used in these experiments are hemizygous for the transgene.

The LamH-BXSB and LamH-NZB strains were generated by backcross of the transgene from the B6 strain ≥9 generations using BXSB or NZB breeders. The LamH-MRL/lpr strain was generated by two serial crosses of the LamH-MRL strain (9 previous backcross generations onto MRL) with MRL/lpr breeders. The BWF1 strain was generated by crossing LamH Tg+ NZB females of backcross generation 13–14 with NZW male breeders, with the resulting progeny used experimentally. All lupus-strain breeders as well as BALB/c allotype controls were from The Jackson Laboratory (Bar Harbor, ME, USA). The age range of mice used in most of these studies was 1.5–9.0 months (mean ages are shown in Table 1, footnote), with the exception of several older BXSB mice used where noted. These studies and procedures were approved by the Duke University and the Durham Veterans Affairs Medical Centers Animal Care and Use Committees.

Transgene determination

Presence of the LamH Ig transgene was determined by PCR using transgene-specific forward and reverse primers:

5’- AGC TGC AAC AGT CTG GAC CTG A -3’ and

5’- GGC CCC AGT AGT CAA AGG TAC CAT C -3’.

Presence of the Fas mutation in LamH-MRL/lpr mice was determined as directed by the Jackson Laboratories standard PCR for the Fas^{lpr} allele.

Cell staining

Single-cell splenocyte, bone marrow, and peritoneal cell suspensions were analyzed by flow cytometry as described [25] using the following fluorescent stains: anti-CD45R/B220-PE and -PerCP, anti-IgMb-FTC, anti-IgMa-PE, anti-CD5-FTC, anti-CD86-RPE, anti-CD21/35-FTC, anti-CD1d-biotin, anti-CD4-PE, anti-CD8-FITC, anti-CD3-FITC and anti-CD138-PE (Becton Dickinson-Pharmingen, San Jose, CA, USA), and anti-CD19-PE, anti-IgM-FTC, anti-lambda-FTC, anti-kappa-PE, anti-CD62L-FTC, anti-MHCII-FTC, and anti-CD23-PE(Southern Biotech, Birmingham, Alabama, USA). Cells were analyzed on a FACSCalibur (Becton Dickinson), and results analyzed using either CellQuest (Becton Dickenson) or FlowJo (Treestar, Ashland, OR, USA). Lymphocytes were gated based on FSC and SSC properties. B cell counts were determined as %B220+ × % lymphocytes × number of splenocytes, except in MRL/lpr mice in which presence of abundant abnormal B220+ T cells required use of CD19 as the B cell marker.

To identify plasma cells and plasmablasts, splenocytes were first stained as above with CD138-PE × B220-PerCP, then fixed in 1% paraformaldehyde containing 0.5% Tween-20 for 30 minutes to permeabilize the cell membrane. Following rinsing, cells were then stained for IgMa, IgG, or total IgM using FITC-conjugated reagents, and fixed again in 1% paraformaldehyde prior to acquisition. BXSB mice used for these experiments were 14–15.5 months of age.

Antibody isotype, allotype, and laminin binding ELISA assays

Ig concentrations and isotype- and allotype-specific laminin binding in serum and in hybridoma and transfectant supernatants were determined by ELISA as described [25] with the following additions: Cell culture supernatant was assayed undiluted in laminin binding assays, and lambda concentration was measured against Ig standard MOPC104e (Sigma) and detected with alkaline-phosphatase conjugated anti-lambda antibody (Southern Biotech).

To assay for laminin binding activity, Immulon II plates were coated overnight at 4C with 10 μg/mL laminin EHS (Sigma). Plates were blocked, rinsed, and detected as above using sera diluted 1:20. Control Ig is anti-laminin mAb A10C supernatant [24]. Results were recorded as the mean sample binding OD to laminin after subtraction of mean OD on diluent-coated plates. For all strains except MRL/lpr, in which IgM-j allotype crossreacts with Tg IgM-a, laminin binding by transgene-encoded Ig was confirmed using biotin-labeled anti-allotype (IgM-a)-specific second-step reagents (BD Biosciences) detected with Streptavidin- alkaline phosphatase (Southern Biotechnology Associates) as above. In MRL/lpr, detection of LamH idiotype-specific serum antibody was performed as described [21].

In vivo cell labeling with BrdU

Newly generated B cells were identified by BrdU incorporation by adding 0.8 mg/ml BrdU (Sigma-Aldrich) to drinking water for 30 days. BrdU-containing water was shielded from light and changed twice weekly. BrdU-labeled splenocytes were identified as described [22].

In vivo LPS stimulation

Four LamH Tg+ NZB mice and four non-Tg controls were injected i.p. with 25–50 μg lipopolysaccharide. Serum was collected after 3 days (n=2/grp) or 8 days (n=2/grp) and assayed for Tg-encoded anti-laminin reactivity as described above.

Hybridoma generation

Hybridomas were derived from unmanipulated or LPS stimulated splenocytes of transgenic mice using standard procedures as described [24]. Supernatants were screened by ELISA for Ig isotype, allotype, and laminin binding as described above, and selected lines subcloned by limiting dilution.

B cell proliferation and differentiation

B cells were purified from RBC-lysed splenocytes using CD43 microbead depletion of non-B cells (Miltenyi Biotec, Auburn, CA, USA). Purified B cells were labeled with 2.5–5.0 μM carboxyfluorescein succinimidyl ester (CFSE, Molecular Probes, Eugene, OR, USA) per the manufacturer's protocol. Labeled cells were cultured at 1.25×10^6 cells/mL in proliferation media (RPMI supplemented with 10% fetal bovine serum, 2 mM L-glutamine, beta-mercaptoethanol, and 100U/mL penicillin-streptomycin), 200 μl per well in a 96-well plate +/− 50 μg/mL lipopolysaccharide (LPS, #L6386, Sigma) or 80 μg/mL goat-anti-mouse IgM $F(ab')_2$ (Fab, Pierce/Thermo Scientific, Rockford, IL, USA). Following 2.5 days in culture, cells were collected and stained with B220-PE and assessed by flow cytometry as detailed above. The percent of divided cells was calculated for the B220+ population using FlowJo.

To assess differentiation into antigen-secreting cells (ASC, plasma cells and plasmablasts), purified B cells were cultured at 1×10^6 cells/mL in 200 μL per well in a 96 well plate +/− 50 μg per mL LPS. Following 3 days in culture, cells were collected and stained for flow cytometry using the CD138 antibody paired with intracellular staining for Ig as described above.

To assess antibody secretion, purified B cells were plated at 1×10^6 cells/mL in 1 mL per well of a 24-well plate, with and without stimulation by LPS as above. Mature supernatants were harvested following 8–10 days of culture and were assayed for laminin binding by ELISA as described above.

Apoptosis and cell death assays

Splenocytes were prepared as described above for flow cytometric staining. One million RBC-depleted splenocytes were rinsed twice in PBS containing 2% FBS, followed by a wash in 1X binding buffer supplied (BD Pharmingen). Cells were stained as directed by the manufacturer using annexin V-FITC, 7-AAD, and either anti-CD19-PE or anti-IgMa-PE. Annexin V and 7-AAD positive cutoffs were set based on the dead cell gate using FSC vs. SSC properties. BXSB mice used in the apoptosis assays were 14–15.5 months of age.

Cloning of MRL/lpr laminin-binding kappa light chain 11.5.E

Poly-A RNA was isolated from hybridoma cells using the RNEasy mini kit (Qiagen, Valencia, CA, USA) followed by the Oligotex mRNA Mini kit (Qiagen). RNA was reverse transcribed using oligo-dT primers and the Universal RiboClone cDNA Synthesis kit (Promega, Madison, WI, USA). The light chain sequence was determined by PCR amplifying cDNA using the degenerate primer, 5'- RRT ATT KTG MTR ACY CAR -3', designed to amplify genes from multiple kappa V gene families, paired with the kappa constant region primer, 5'-CTG CTC ACT GGA TGG TGG GA-3'. Amplified products were then sequenced directly using the kappa constant region primer.

Forward and reverse primers containing *Not I* and *Sal I* restriction sites, respectively, were designed for amplification of clone 11.5.E VκJκ and cloning into kappa-targeting vector (KTV) generously provided by Dr. Klaus Rajewsky via Dr. Thereza Imanishi-Kari (Tufts University). The forward primer (5'- CAT GCG GCC GCA GGA AAA CAA GAA ACA GAT AAT GC -3') lies 689 bp upstream of framework region 1 and was designed using

mouse genomic BLAST (http://blast.ncbi.nlm.nih.gov/Blast.cgi) by incorporating upstream sequence of the germline Vκ gene (GenBank accession NT_039343) most closely matching the sequence of 11.5.E. The sequence of the reverse primer (5'- ATA GTC GAC AGA CCA CGC TAC CTG CAG TCA GAC -3'), which lies 292 bp downstream of Jκ5, was provided with vector KTV. The 2.3 kb amplicon was gel-purified and cloned into vector pCR2.1-TOPO using the TOPO TA Cloning kit (Invitrogen, Carlsbad, CA). The 5', 3', and VκJκ regions were verified by sequencing with vector- and Vκ-specific primers. This 2.3 kb fragment containing the 11.5.E L chain and all upstream regulatory sequences was excised from vector pCR2.1-TOPO by digestion with *Not I* and *Sal I* (New England Biolabs, Beverly, MA) and ligated with *Not I/Sal I*-digested vector KTV using T4 DNA ligase (New England Biolabs).

Transfection

The light chain from laminin-binding Ig 11.5.E, cloned into the KTV expression vector, was cotransfected with the LamH (transgenic) heavy chain into lambda L chain-expressing J558L cells [26] by electroporation using a BioRad Gene Pulser. The LamH/J558L transfectant Ig does not bind laminin [20]. Ten million cells were electroporated in 300 uL PBS along with 10 ug linearized plasmid DNA and 1 ug of the coselectable G418-resistance marker KJ-1 [27], and selected using 400 ug/mL G418.

Sequencing and sequence alignment

LamH H chain DNA from hybridoma clones was sequenced at the Duke University DNA Analysis Facility following PCR amplification for the transgene as described above. The 11.5.E H chain was additionally sequenced following PCR amplification using primer set: 5'- TGT GAA CAT AGC CC AGA GTG AC -3' with 5' GAC TCA CCT GAG GAG ACT GTG AG – 3'.

Light and heavy chain family designations and homologies were determined using the ImMunoGeneTics (IMGT) Information system website at www.imgt.org (28).

Statistical analyses

All data are shown as mean values ± standard deviation (SD). Comparisons between two groups were performed using the nonparametric Wilcoxon test. Comparisons between paired samples in the BrdU assay were performed using the paired t-test. Analyses were performed with JMP software (SAS Institute, Cary, NC). A value of $p < 0.05$ was considered to be significant.

Results

Lack of transgenic anti-laminin antibody in LamH Ig Tg BXSB, BWF1, and NZB mice

Endogenous BXSB, BWF1, and NZB IgM is b-allotype, making expression of the Tg IgM a-allotype easily discernable in these strains. Because the MRL/lpr endogenous j-allotype IgM crossreacts with IgMa-detecting reagents, findings in this strain are considered separately. Results for males and females are presented together, except where stated otherwise.

In mice carrying the LamH Ig Tg on the BXSB, BWF1, or NZB autoimmune backgrounds, we found negligible circulating transgenic anti-laminin antibody (Figure 1A). This absence of serum Tg anti-laminin autoreactivity occurs despite the presence of readily detectable serum Tg-encoded antibody (a-allotype IgM) in all transgenic mice of each strain (Figure 1B). In the BXSB strain, serum IgMa levels were significantly higher in male Tg+ as compared to female Tg+ mice (39.2 ± 25.0 and 26.6 ± 24.9 μg/ml, respectively, $p<0.05$).

LamH Tg is a conventional, not site-directed, IgM Tg, and the likelihood of class-switched Tg-encoded IgG is quite low. To examine whether class-switched Tg-encoded IgG was detectable in these subjects, we tested sera for anti-laminin IgG. Of 42 sera tested [NZB: 10 Tg+, 4 non-Tg; BXSB: 9 Tg+, 5 non-Tg; BWF1: 9 Tg+, 5 non-Tg], the large majority were negative for anti-laminin IgG. The 4 positive sera, including one Tg+ mouse (NZB,) and three non-Tg mice (2 BXSB, 1 NZB), had measurable but low level anti-laminin IgG.

To further investigate anti-laminin autoantibody production at the single cell level, hybridomas were generated by fusion of unstimulated splenocytes from 2–3 Tg+ BWF1, BXSB, and NZB mice. These fusions yielded few hybridomas, including 12 IgM-producing clones from Tg+ BXSB, 2 from Tg+ NZB, and 3 from Tg+ BWF1. None of these spontaneous hybridomas produced laminin-binding antibodies. These outcomes are reminiscent of our previously reported inability to recover anti-laminin monoclonal antibodies from either tolerant LamH Ig Tg B6 mice or LamH/Vk8Jk5 H+L Ig Tg mice [21, 22], and in striking contrast to the numerous anti-laminin Tg mAb recovered from the aberrant M07 LamH Ig Tg line with disabled surface Tg expression in which B cells are not subject to BCR-mediated tolerizing signals [20].

Depletion of Tg+ anti-laminin B cells in four lupus strains

In BXSB, BWF1, NZB, and MRL/lpr backgrounds, transgenic mice had significantly fewer splenic B cells than their non-transgenic counterparts (Figure 2). Overall, the total number of splenic B cells per mouse was reduced 76–83% (Table 1). This approaches the 88–89% reduction seen in the Tg B6 strain [21, 22], including in Tg B6 mice carried concurrently in our colony (unpublished data). BXSB males showed the greatest reduction in B cell numbers, with 90% fewer spleen B cells in male Tg+ than male non-Tg mice (not shown). In the three strains expressing b-allotype endogenous IgM (BXSB, BWF1, NZB), the majority of surviving splenic B cells expressed exclusively transgene a-allotype IgM (Table 1A and Figure 3A).

Tg+ males had significantly fewer splenic B cells than Tg+ females in two strains: BXSB (7.3 ± 3.1 vs. 11.9 ± 5.4 million, $p<0.05$), and NZB (2.9 ± 1.5 vs. 4.3 ± 1.4 million, $p<0.05$). There were no differences between the sexes in B cell counts in Tg+ BWF1 or MRL/lpr mice.

The reduction in B cell number was also observed in the bone marrow (Table 1B and Fig. 3B). Tg+ BXSB, BWF1, and NZB mice had a significantly lower percentage of IgM+ B cells in bone marrow than did their non-transgenic counterparts. These results are similar to our observations in Tg B6 mice [22]. The lower percentage IgM+ B cells in Tg+ MRL/lpr mouse bone marrow did not reach statistical significance.

Evidence of secondary Ig rearrangements in anti-laminin B cells in BWF1, BXSB, and NZB mice

In Tg+ mice in the BWF1, BXSB, and NZB backgrounds, endogenous heavy chain (b-allotype IgM) was coexpressed on the surface of a minority of B cells (Figure 3A and Table 1A), indicating secondary rearrangements at the endogenous loci despite presence of the rearranged Tg H chain in a subset of cells. Endogenous IgMb was similarly generally excluded on the surface of B cells in Tg B6 mice (21). Among Tg+ mice, only BXSB demonstrated a significant sex-bias in spleen B cell expression of endogenous b-allotype IgM ($9.9 \pm 4.2\%$ for males, $14.1 \pm 4.6\%$ for females, $p<0.05$). Endogenous IgMb was also detected among a subset of hybridoma supernatants: 7 of 12 hybridomas derived from Tg+ BXSB mice secreted endogenous IgM-b, of which 4 coexpressed Tg IgMa, and endogenous IgMb was coexpressed with Tg by one of three Tg+ BWF1 and both Tg+ NZB hybridomas.

In the BXSB and NZB backgrounds, a significantly higher proportion of splenic B cells expressed lambda light chains in Tg+ mice as compared to their non-Tg counterparts (Table 1A), suggesting multiple attempts at light chain rearrangements in these strains. Lambda light chains were expressed by 3 of 12 Tg+ BXSB-derived hybridomas. In contrast, Tg+ BWF1 splenocytes had significantly lower lambda light chain expression than non-Tg BWF1 B cells (Table 1A), and none of 3 BWF1 hybridomas secreted lambda-expressing Ig.

B cell proliferation, differentiation, Ab secretion, in vivo turnover, surface marker expression, and apoptosis by residual Tg+ B cells in lupus strains

All LamH Ig Tg+ mice from BWF1, BXSB, and NZB backgrounds have a residual population of Tg+ (IgMa+) B cells (Figure 3), yet no Tg anti-laminin activity is recovered in serum from these strain. This suggests that the residual Tg+ B cells are either autoreactive and anergic, as previously suggested for LamH Tg+ B cells on the B6 and MRL backgrounds [21], or result from pairing of LamH Tg+ with endogenous light chains that do not result in autospecificity. To assess whether the B cells from LamH mice exhibit features of anergy, we examined their responsiveness to exogenous stimulation ex vivo, their turnover rate in vivo, and expression of surface markers previously reported to be altered on LamH anergic B cells [21, 22].

In proliferation assays using purified B cells from NZB mice, significantly fewer B cells from Tg+ mice proliferated in response to IgM receptor crosslinking compared to cells from non-Tg mice (Figure 4A). In contrast, studies with BXSB mice showed a significantly higher proportion of proliferated cells in response to receptor crosslinking among B cells purified from Tg+ as compared to non-Tg mice (Figure 4B). BXSB Tg+ B cells also hyperproliferated in response to LPS stimulation (Figure 4B). This was observed in B cells from both male and female Tg+ BXSB (not shown). In BWF1 mice, no differences were observed between purified Tg+ and non-Tg B cells in proliferative response to either stimulus (Figure 4C). Whereas these experiments do not allow direct comparison to our previous experiments with B6 Tg B cells in which we observed hypoproliferation of B cells within whole splenocyte preparations [21], they do indicate lupus strain-dependent differences in proliferative responses of isolated B cells.

To assess the capacity of Tg+ B cells to secrete autoantibodies, purified B cells from Tg+ mice were incubated with medium alone or medium supplemented with lipopolysaccharide. Tg+ NZB B cells were unique in that whereas they produced little autoantibody in culture without stimulation, they produced high levels of Tg-encoded anti-laminin Ig after culture with LPS (Figure 5). In contrast, assay of culture supernatants from Tg+ BXSB and Tg+ BWF1 B cells revealed undetectable or only low levels of Tg-encoded anti-laminin Ig, with or without LPS stimulation (Figure 5), similar to results with B cells from Tg+ B6 and MRL mice [21, 22]. The presence of Tg anti-laminin reactivity in LPS-stimulated NZB B cell culture supernatants did not result from increased overall levels of secreted IgMa: LPS-stimulated NZB Tg+ B cell cultures contained, on average, 4.0 ± 4.7 μg/mL IgMa. This is in contrast to considerably higher IgMa levels seen in LPS-stimulated BXSB Tg+ cultures which had an average of 19.4 ± 32.7 μg/mL IgMa. Insufficient sample precluded IgMa concentration analysis for BWF1 supernatants.

To assess in vivo B cell turnover, cells were labeled with BrdU over a 30 day exposure period. Tg+ NZB mice had a significantly higher percentage of BrdU-labeled splenic B cells than did than non-Tg NZB mice (Figure 6). This is reminiscent of our previously reported observations in B6 mice, in which BrdU labeling in Tg mice (approximately 60% of B cells at 30 days) was more than double that of their non-Tg counterparts [22]. In contrast, there was no difference in B cell turnover between Tg+ and non-Tg BXSB mice (Figure 6).

Splenic B cells from Tg+ mice of BWF1, BXSB, and NZB mice all showed a significant increase in surface density of CD5 (Table 2). CD23 was significantly decreased in Tg+ vs non-Tg mice on the BXSB and NZB mice, and showed a similar trend in BWF1 mice ($p<0.07$) (Table 2 and Figure 7). Tg+ NZB mice had increased expression of CD86 and decreased surface Ig density compared to their non-Tg NZB counterparts, a surface marker phenotype that most closely paralleled that of anergic LamH Tg+ B cells in the B6 non-autoimmune background [22]. Surface Ig density was also decreased on Tg+ BWF1 B cells, and both Tg+ NZB and BWF1 B cells had significantly decreased frequency of CD21/35 relative to non-Tg counterparts. In contrast, B cells in Tg+ BXSB mice were unique in demonstrating significantly increased CD21/35 (Table 2 and Figure 7) and high density B cell surface Tg+ IgMa expression (Figure 3). Co-staining of splenic B cells from older Tg+ BXSB mice with CD21 and CD1d confirms a prominent marginal zone B cell subset not observed in non-Tg BXSB mice (Figure 7C). Similar staining in NZB mice did not identify significant differences between Tg and nonTg mice (not shown).

Because NZB and BXSB Tg+ mice have unique B cell phenotypes with differential ability to produce Tg autoIg, we determined the ability of activated B cells in Tg+ mice to differentiate into antibody secreting cells (ASC) by assessing expression of CD138. We analyzed CD138 expression both on freshly isolated spleen lymphocytes and on purified B cells after 3 days in culture with or without LPS stimulation. Results show that the percentage of CD138+ cells among lymphocytes did not differ between Tg+ and non-Tg mice in NZB mice (1.9 ± 0.6% vs 1.6 ± 0.4%, respectively, p=NS) or in BXSB mice (1.6 ± 0.2% vs 1.2 ± 0.3%, respectively, p=NS). These findings indicate that at least a subset of Tg + B cells differentiate to ASC in vivo in both lupus strains. These results further suggest that ASC are enriched among B cell populations in Tg+ mice, because Tg+ mice in both strains have markedly fewer total B cells as determined by B220+ staining (Figure 2, Table 1). CD138+ cells were also enriched in 3 day LPS cultures of purified B cells from Tg+ mice compared to cultures of cells from non-Tg mice of both strains: 30.2 ± 0.4% vs. 16.6 ± 6.0%, respectively, for Tg+ vs non-Tg cells from NZB mice, p=<0.05, and 16.3 ± 5.0% vs 5.7 ± 2.6%, respectively, in BXSB mice, p=<0.05, n=3–6 mice/group. Tg IgMa+ ASC were readily detected in these LPS-induced cultures: 30.8% and 50.1% of CD138+ cells were IgMa+ in NZB and BXSB cultures, respectively.

Because apoptosis plays important role in B cell selection and regulation and tolerance in LamH Tg may be mediated by peripheral mechanisms such as clonal deletion and anergy (in addition to editing and deletion in the bone marrow), we assessed in NZB and BXSB mice whether freshly harvested splenic B cells from Tg+ mice have evidence of enhanced apoptosis relative to B cells of their wildtype counterparts. Annexin staining showed that the proportion of spleen CD19+ B cells undergoing apoptosis was significantly higher in Tg+ as compared to non-Tg mice in both NZB and BXSB mice (Figure 8). BXSB and NZB Tg+ B cells displayed approximately 2.1-fold and 1.6-fold, respectively, higher degrees of B cell apoptosis than did their wildtype counterparts ($p<0.05$, Tg+ vs non-Tg, for both strains).

Rare escape of anti-laminin B cells in MRL/lpr mice

Because MRL/lpr mice have j allotype IgM, which cross-reacts with the anti-IgMa detection reagent, we cannot identify the transgenic heavy chain by IgMa allotype-specific staining in this strain. Alternatively, sera were interrogated with an anti-idiotype mAb that recognizes the LamH Tg H chain [29], revealing LamH-Id+ Ig in 35.7% of (n=14) Tg+ MRL/lpr mouse sera and in none of 15 non-Tg MRL/lpr mice. While anti-laminin IgM are detected in the serum of a subset of both Tg+ and non-Tg mice, only two of 14 MRL/lpr Tg+ mice have both anti-laminin and LamH-Id+ Ig in their serum, suggesting that anti-laminin Tg B cells may escape regulation in approximately 14% of MRL/lpr mice.

Flow cytometric analysis revealed evidence of H chain editing in a small subset of MRL/lpr Tg+ splenic B cells, manifest as low level surface expression of endogenous IgD (14.7 ± 13.4% of B cells, n=10, compared to 71.2 ± 16.6%, n=8, for non-Tg MRL/lpr counterparts.) Surface lambda expression was negligible on Tg+ MRL/lpr splenocytes. A limited analysis of MRL/lpr B cell surface markers showed no significant difference in spleen B cell CD5+ expression in Tg+ compared to non-Tg mice.

To further explore the origin of autoreactivity in Tg+ MRL/lpr, hybridomas were generated by fusion of unstimulated splenocytes (n=4 Tg+ spleens) or splenocytes stimulated for 24 hours with LPS prior to fusion (n=3 Tg+ spleens), and cloned by limiting dilution. Of 50 IgM-producing hybridoma lines recovered (38 from unstimulated, 12 from LPS-stimulated), a single IgM,kappa producer derived from unstimulated splenocytes, termed 11.5.E, generated anti-laminin Ig in culture. This clone was sequenced and shown to contain a mutation altering one amino acid (Phe for Tyr) in the Tg-encoded heavy chain antigen-binding CDR3 region (Fig 8A).

Non-critical H chain mutation in MRL/lpr anti-laminin Ig

The CDR3 mutation of the Tg H chain in hybridoma 11.5.E raised the possibility that the parent B cell of this clone was not autoreactive when developing in the bone marrow, such that its fate was not regulated by central tolerance mechanisms, but rather that it acquired laminin autospecificity after H chain mutation in the periphery. To investigate this possibility, the 11.5.E light chain was cloned and co-expressed with the unmutated LamH Tg H chain using electroporation into a murine myeloma cell line. Concentration-matched ELISA showed that both the mutated 11.5.E H chain and the unmutated LamH Tg generate a laminin binding autoantibody when paired with the 11.5.E L chain (OD_{405} 0.505 ± 0.003 and 0.260 ± 0.030, respectively, with concurrent OD_{405} 0.322 ± 0.076 for positive control H50-9 IgG at 10 ug/ml).

Sequence analysis of the 11.5.E L chain (GenBank accession number JQ513389) revealed it to be a member of the IGKV4 (previous Vk4/5) Vk gene subgroup paired with an IGKJ2 gene segment. Although there is no comparable published reference MRL/lpr-derived germline kappa sequence, GenBank homology searching provided sequences from numerous MRL/lpr-derived mAb that express IGKV4 genes. Assembly of a consensus sequence suggests that the 11.5.E L chain contains one framework 1 and two CDR region missense mutations (Fig. 8B).

T cell numbers and CD4/CD8 ratio in anti-laminin Ig Tg mice

To assess the potential impact and interaction of the LamH Ig Tg and T cells in the lupus strains, CD3+ spleen T cells and CD4/CD8 subsets were enumerated (Figure 10). The results show that total T cell numbers are significantly reduced in Tg BXSB and Tg BWF1 mice, and the ratio of CD4 and CD8 T cells is significantly reduced in Tg mice in all three strains. We previously reported a significantly reduced T cell population in B6 Tg mice, whereas the CD4/CD8 ratio was not different from non-Tg mice in B6 [21].

Discussion and Conclusions

To examine if and how different constellations of lupus susceptibility loci differentially modify autoreactive B cell fate, we established the same autoreactive anti-laminin H-chain dominant Ig Tg in each of four classic murine lupus strains, BXSB, BWF1, MRL/lpr and NZB, genetically predisposed to aggressive systemic autoimmunity. Our results indicate that although B cell reactivity to laminin is regulated in all strains, Tg B cells meet a distinct fate in each. This includes ready recovery of anti-laminin Tg Ig from LPS-stimulated cultured

NZB Tg+ B cells and acquisition of a unique CD21hi/IgMhi phenotype by Tg+ B cells in BXSB mice. CD1d staining confirms expansion of the marginal zone subset in Tg+ BXSB. Central deletion of most anti-laminin B cells appears to be grossly intact in each strain, because Tg+ mice have 4–6 fold fewer splenic B cells than their non-Tg counterparts, and in the BXSB, BWF1, and NZB strains this is accompanied by significantly fewer IgM+ B cells in bone marrow. This bone marrow phenotype did not reach statistical significance in MRL/lpr Tg+ mice, but may have been obscured in part by the relative paucity of B cells in the MRL/lpr mice, a strain that develops an unusual CD4-CD8- T cell expansion. The B depletion mirrors that observed in nonautoimmune B6 mice carrying the LamH Ig Tg [21], in whom profound central deletion with a requirement for kappa editing for Tg B cell rescue was previously shown [22].

Our findings also suggest distinct abnormalities in Tg B cell deletion in two lupus strains, BXSB and NZB. Unexpectedly and seemingly paradoxically, BXSB Tg+ male mice, which harbor the y-chromosome-linked autoimmune accelerator locus *yaa*, have the highest proportion of B cell depletion of any strain examined, with 10-fold fewer spleen B cells than non-Tg BXSB males. Moreover, BXSB Tg+ males have significantly fewer B cells than BXSB Tg+ females, suggesting that the *yaa* translocation facilitates the deletion process, possibly by lowering BCR signaling thresholds [30]. In this regard, Izui and colleagues have proposed that a yaa-linked reduction in the B cell threshold for activation underlies the spontaneous activation of anti-red blood cell Tg B cells observed in B6.yaa male mice expressing the 4C8 Ig Tg [31]. The molecular mechanism by which *yaa* might promote B cell deletion, or hinder the editing machinery that would otherwise rescue anti-laminin B cells destined for deletion, is unclear. *Yaa* carries a translocated duplication of Toll-like receptor (TLR) 7 [32, 33], as well as at least 16 additional as yet unidentified genes [34]. TLR7 is suspected of modulating autoreactive B cell fate at the point of early cell development [35], however, its expression and function in the bone marrow is less well characterized than cell surface-expressed TLRs. Alternatively, TLR7 or other yaa gene products may preferentially influence extrinsic B cell factors that limit peripheral B cell survival. It is also possible that the effect is yaa-independent, but rather due to sex hormones or other sex-related influences that impact B cell number in this strain. Further studies should resolve these questions, including the requirement for a superimposed autoimmune BXSB background.

In contrast, our findings in NZB Tg mice suggest that central deletion pathways are partially defective in the NZB strain. NZB Tg mice are unique among the examined strains in their production of high levels of Tg anti-laminin IgM after in vitro stimulation with LPS. The induction of serum Tg anti-laminin Ig in a subset of NZB Tg mice injected with LPS suggests that this loss or reversal of tolerance is not prevented by in vivo regulatory pathways. The impact on NZB disease will require additional studies. These observations do suggest that a subset of anti-laminin Tg B cells escape central deletion in NZB to populate the spleen; absence of antilaminin Tg Ig in serum or supernatants of unstimulated B cells indicates that they are not spontaneously activated in vivo. Whereas the molecular mechanism underlying bone marrow escape in NZB is unknown, precedence for genetically determined defects in central B cell deletion leading to increased numbers of peripheral autoreactive B cells come from recent reports in patients and mice deficient in interleukin-1 receptor-associated kinase 4 (IRAK-4), myeloid differentiation factor 88 (MyD88), or activation-induced cytidine deaminase (AID), and in individuals carrying the PTPN22 R620W autoimmune risk allele [36–39]. Not all defects lead to full fledged autoimmunity with spontaneous serum autoantibody production, highlighting the importance of downstream checkpoints. It is possible that defective central deletion in NZB also contributes to the loss of B cell tolerance to RBC antigens and development of autoimmune hemolytic anemia in NZB mice, noting that in nonautoimmune B6 mice, B cells bearing the

NZB-derived 4C8 anti-RBC Ig Tg are predominantly controlled by central deletion [40, 41]. Whereas a subset of peritoneal sequestered CD5+ B-1a anti-RBC cells escape regulation in the B6 4C8 Tg model, this escape route is not apparent in our NZB LamH Tg mice (data not shown).

Whether the surviving anti-laminin Tg B cells are subject to further dysregulation in the NZB periphery will require further study. The frequency of laminin-specific cells among residual Tg splenocytes is not readily determined, as soluble laminin does not engage the Tg and cannot be used as probe [21]. It is of interest that the majority of surviving NZB Tg spleen B cells retain several features consistent with anergy as described previously in B6 LamH Tg mice. NZB Tg B cells express significantly lower levels of surface Ig, CD23, and CD21 and increased CD86 and CD5 compared to their non-Tg counterparts. NZB Tg B cells also have increased turnover in vivo and hypoproliferate in response to BCR crosslinking. If the surviving NZB Tg anti-laminin B cells are anergic, the recovery of laminin autoreactivity suggest that anergy is reversible with LPS. The NZB Tg B cell phenotype is somewhat reminiscent of anti-hen egg lysozyme (HEL) Ig Tg carried on NZB, which is to our knowledge the only other Ig Tg studied in NZB. Whereas anti-HEL Tg B cells are anergic in non-autoimmune B6 mice that also carry the Tg for soluble HEL (neoself Ag) [42], in NZB mice carrying both Tg, anti-HEL B cells retain an anergic phentoype yet mice nonetheless spontaneously develop high serum titers of Tg autoantibody [43]. NZB-derived defects in anergic cell survival and activation due to T cell help, elevated BAFF levels, and intrinsic cell abnormalities are hypothesized. Further studies should elucidate the developmental and functional state of our NZB anti-laminin B cells.

Residual Tg B cells in BXSB mice are unique in that they lack most characteristics of anergic cells observed in the other strains, including B6 and BWF1. Moreover, they hyperproliferate to both LPS stimulation and to B cell receptor crosslinking, demonstrate a normal in vivo lifespan by BrdU labeling, and express IgMhi/CD21hi/CD23lo/CD1d+ markers indicating marginal zone (MZ) B cell expansion. These cells are observed in both male and female BXSB Tg mice, suggesting independence from *yaa* locus influences previously reported to mediate MZ B cell depletion [30, 44]. Thus BXSB genetic influences divert surviving LamH Ig Tg cells from functional anergy as observed in B6 mice to a longer-lived population capable of exaggerated responses to LPS and BCR stimulation. It is notable that expansion of a MZ-like B cell population was also observed in male BXSB mice bearing the trinitrophenyl/ ssDNA/ dsDNA-reactive Sp6 Ig Tg, irrespective of the presence of *yaa* [30]. Abnormal expansion or biology of murine MZ B cells, major autoIg producers [45] known to respond robustly to TLR ligands [46], has been linked to disease in some models [47–54]. Of note, the hyperproliferation of our BXSB Tg B cells to B cell receptor crosslinking is unusual for MZ B cells, which normally undergo apoptosis in response to this stimulus [46]. These studies extend our preliminary findings in early generation BXSB Tg backcross mice [55], and shed light on the fate of autoreactive B cells in a background about which little was previously known.

Because BXSB Tg+ and NZB Tg+ mice have the most distinct B cell phenotypes and anti-laminin Ig are induced only from NZB B cells, we sought evidence of other differences in these two Tg+ strains. Annexin staining shows that B cells from both Tg+ strains display higher levels of apoptosis than do their non-Tg counterparts, and the fold increase is similar between strains. There is no overt strain-specific defect in ability to differentiate to ASC, either in vivo or in response to LPS in vitro, that explains the differential cell fate and autoIg production. Future studies can determine the B cell subsets undergoing enhanced apoptosis, the nature of affected B cell selection pathways, and the contribution of T cells, other immune cell populations, or specialized spleen microenvironments (such as MZ or germinal center), as suggested in other model systems [56]. The depressed CD4/CD8 T cell ratio is

observed in both NZB and BXSB Tg+ mice, as well as in BWF1. A similar phenomenon is reported in BWF1 mice bearing an anti-DNA Ig Tg [57]; in this model, altered T cell subsets and abrogation of lupus nephritis are attributed to depletion of endogenous (non-Tg) BWF1 B cells that normally promote accumulation of activated and memory T cells. B cells are also known to be critical for spleen T cell development [58]. Future experiments can dissect underlying cellular and molecular mechanisms, including use of ex vivo and in vivo adoptive transfer and mixed bone marrow chimeras to replenish endogenous subsets potentially altered by the Ig Tg model.

MRL/lpr Tg have yet a different phenotype, in that rare Tg anti-laminin autoIg can be recovered as mAb from unstimulated splenocytes, suggesting defects in peripheral and possibly central tolerance. However, Tg anti-laminin Ig appear to be rare in serum and among hybridomas, and their frequency is not increased by antigen-in-adjuvant immunization (data not shown) or LPS stimulation prior to fusion, suggesting a stochastic or environmental contribution to loss of tolerance in individual MRL/lpr mice. Tracking of other autoIg Tgs in the MRL/lpr background has identified a variety of abnormalities, including an environmental component, failure to sustain developmental arrest and anergy, altered availability of T cell help, peripheral re-editing, defective marginal zone sequestration or B-1 differentiation, and extrafollicular expansion and activation [59–62]. Future studies can dissect factors that permit survival and activation of anti-basement membrane B cells in this strain.

We find little phenotypic difference between BWF1 and B6 LamH Tg+ mice. B cell tolerance to laminin is preserved in BWF1 despite the genetic susceptibility to aggressive lupus with nephritis characteristic of BWF1 and 50% contribution of NZB to the genome. B cell tolerance to another self-Ag, dsDNA, is variably preserved in BWF1 expressing different anti-DNA Ig H chain Tgs, suggesting complex influences of Ag and Tg structure in BWF1 lupus [63–66].

It is possible that the outcomes we observe are affected in part by the nature of the LamH Tg itself. IgG switch is not possible using a conventional IgM Tg except in unusual circumstances, such that peripheral tolerance mechanisms that specifically control IgG-switched B cells will not be engaged in our model. The LamH Ig Tg construct also does not include IgD. However, it has been shown that absence of IgD does not alter central B cell deletion or editing [67], probably because mIgD is first expressed on mature cells, and mice rendered IgD-deficient have only subtle defects in humoral immunity and variable B cell numbers [68, 69]. IgD is drastically downregulated on activated B cells, such that effects at late stages of cell differentiation seem unlikely. Finally, it is possible that alterations in primary B cell repertoires contribute in part to the unique phenotypes observed in these strains. The LamH Ig Tg generates a polyclonal B cell population by pairing with endogenous L chains, many of which generate anti-laminin Ig when combined with the LamH H chain on the B6 background [20]. It is thus notable that NZB, BWF1, and MRL/lpr mice share with NOD mice parts of the rare Igkappa b-haplotype that may predispose to autoimmunity, including Vk gene polymorphisms not carried in common nonautoimmune strains [70, 71]. MRL/lpr mice additionally carry the distinct D gene repertoire of the IgH j-haplotype, which may also impact the primary repertoire [72, 73].

In summary, we observed distinct fates of the anti-laminin Ig Tg when expressed on different strains with aggressive lupus. Several of our findings are unexpected, and suggest previously unsuspected influences from autoimmune susceptibility. This includes easy recovery of Tg autoIg from NZB, a strain considered to have the least aggressive lupus of the group, and an enriched CD21hi/IgMhi/CD1d+ MZ population of B cells in BXSB mice. Further investigation will be required to dissect the molecular basis of these differences,

each of which may be involved in escape from tolerance leading to lupus. Two of our models are unique to the field, as there is no published report of a deletional or disease-derived autoIg Tg model within NZB, a strain rarely used for Ig Tg studies, or of in depth study of any autoIg Tg within BXSB, despite their critical importance to the field. The major lupus strains collectively provide an integrated system to model human lupus genetic heterogeneity. Ultimately, it is hoped that dissection of mechanisms in these models will provide insight into the diversity of autoimmune responses, and the basis of differences in therapeutic response, observed in human SLE, and provide insight into new potential druggable targets for personalized intervention in this debilitating and clinically heterogeneous autoimmune disease.

Acknowledgments

We thank J. Michael Cook, PhD and the Duke University Comprehensive Cancer Center Flow Cytometry Shared Resource and the Duke University DNA Analysis Facility. We thank Erica K. Ungewitter and Bolin LindaYe for technical assistance.

Declaration of Interest:

This work was supported by Award Number R01DK047424 from the National Institute Of Diabetes And Digestive And Kidney Diseases (MHF) and the DVAMC Research Service.

Abbreviations used

Tg	transgene/transgenic
BWF1	(NZBxNZW)F1
HEL	hen egg lysozyme
ASC	antibody secreting cell
MZ	marginal zone

References

1. Harley IT, Kaufman KM, Langefeld CD, Harley JB, Kelly JA. Genetic susceptibility to SLE: new insights from fine mapping and genome-wide association studies. Nature reviews Genetics. 2009; 10(5):285–290.
2. Ramos PS, Brown EE, Kimberly RP, Langefeld CD. Genetic factors predisposing to systemic lupus erythematosus and lupus nephritis. Seminars in nephrology. 2010; 30(2):164–176. [PubMed: 20347645]
3. Kono DH, Theofilopoulos AN. Genetics of SLE in mice. Springer Semin Immunopathol. 2006; 28(2):83–96. [PubMed: 16972052]
4. Morel L. Genetics of SLE: evidence from mouse models. Nat Rev Rheumatol. 2010; 6:348–357. [PubMed: 20440287]
5. Pathak S, Mohan C. Cellular and molecular pathogenesis of systemic lupus erythematosus: lessons from animal models. Arthritis research & therapy. 2011; 13(5):241. [PubMed: 21989039]
6. Kyogoku C, Langefeld CD, Ortmann WA, Lee A, Selby S, Carlton VE, et al. Genetic association of the R620W polymorphism of protein tyrosine phosphatase PTPN22 with human SLE. Am J Hum Genet. 2004; 75(3):504–507. [PubMed: 15273934]
7. Kozyrev SV, Abelson AK, Wojcik J, Zaghlool A, Linga Reddy MV, Sanchez E, et al. Functional variants in the B-cell gene BANK1 are associated with systemic lupus erythematosus. Nature genetics. 2008; 40(2):211–216. [PubMed: 18204447]
8. Cunninghame Graham DS, Graham RR, Manku H, Wong AK, Whittaker JC, Gaffney PM, et al. Polymorphism at the TNF superfamily gene TNFSF4 confers susceptibility to systemic lupus erythematosus. Nature genetics. 2008; 40(1):83–89. [PubMed: 18059267]

9. Gateva V, Sandling JK, Hom G, Taylor KE, Chung SA, Sun X, et al. A large-scale replication study identifies TNIP1, PRDM1, JAZF1, UHRF1BP1 and IL10 as risk loci for systemic lupus erythematosus. Nature genetics. 2009; 41(11):1228–1233. [PubMed: 19838195]
10. Cunninghame Graham DS, Morris DL, Bhangale TR, Criswell LA, Syvanen AC, Ronnblom L, et al. Association of NCF2, IKZF1, IRF8, IFIH1, and TYK2 with systemic lupus erythematosus. PLoS genetics. 2011; 7(10):e1002341. [PubMed: 22046141]
11. Zhou XJ, Lu XL, Nath SK, Lv JC, Zhu SN, Yang HZ, et al. Gene-gene interaction of BLK, TNFSF4, TRAF1, TNFAIP3, and REL in systemic lupus erythematosus. Arthritis and rheumatism. 2012; 64(1):222–231. [PubMed: 21905002]
12. Chung SA, Taylor KE, Graham RR, Nititham J, Lee AT, Ortmann WA, et al. Differential genetic associations for systemic lupus erythematosus based on anti-dsDNA autoantibody production. PLoS genetics. 2011; 7(3):e1001323. Epub 2011/03/17. [PubMed: 21408207]
13. Hall SW, Cooke A. Autoimmunity and inflammation: murine models and translational studies. Mammalian genome : official journal of the International Mammalian Genome Society. 2011; 22(7–8):377–389. Epub 2011/06/21. [PubMed: 21688192]
14. Sabbaga J, Line SRP, Potocnjak P, Madaio MP. A murine nephritogenic monoclonal anti-DNA autoantibody binds directly to mouse laminin, the major non-collagenous protein component of the glomerular basement membrane. Eur J Immunol. 1989; 19:137–143. [PubMed: 2784103]
15. Foster MH, Sabbaga J, Line SRP, Thompson KS, Barrett KJ, Madaio MP. Molecular analysis of nephrotropic anti-laminin antibodies from an MRL/lpr autoimmune mouse. J Immunol. 1993; 151:814–824. [PubMed: 8335911]
16. Ben-Yehuda A, Rasooly L, Bar-Tana R, Breuer G, Tadmor B, Ulmansky R, et al. The urine of SLE patients contains antibodies that bind to the laminin component of the extracellular matrix. J Autoimmun. 1995; 8:279–291. [PubMed: 7612153]
17. Amital H, Heilweil M, Ulmansky R, Szafer F, Bar-Tana R, Morel L, et al. Treatment with a laminin-derived peptide suppresses lupus nephritis. J Immunol. 2005; 175(8):5516–5523. [PubMed: 16210660]
18. Amital H, Heilweil-Harel M, Ulmansky R, Harlev M, Toubi E, Hershko A, et al. Antibodies against the VRT101 laminin epitope correlate with human SLE disease activity and can be removed by extracorporeal immunoadsorption. Rheumatology (Oxford). 2007; 46(9):1433–1437. [PubMed: 17686790]
19. Zhen QL, Xie C, Wu T, Mackay M, Aranow C, Putterman C, et al. Identification of autoantibody clusters that best predict lupus disease activity using glomerular proteome arrays. J Clin Invest. 2005; 115(12):3428–3439. [PubMed: 16322790]
20. Fitzsimons MM, Chen H, Foster MH. Diverse endogenous light chains contribute to basement membrane reactivity in nonautoimmune mice transgenic for an anti-laminin Ig heavy chain. Immunogenetics. 2000; 51:20–29. [PubMed: 10663558]
21. Rudolph EH, Congdon KL, Sackey FN, Fitzsimons MM, Foster MH. Humoral autoimmunity to basement membrane antigens is regulated in C57BL/6 and MRL/MpJ mice transgenic for anti-laminin Ig receptors. J Immunol. 2002; 168:5943–5953. [PubMed: 12023401]
22. Brady GF, Congdon KL, Clark AG, Sackey FN, Rudolph EH, Radic MZ, et al. Kappa editing rescues autoreactive B cells destined for deletion in mice transgenic for a dual specific anti-laminin Ig. J Immunol. 2004; 172(9):5313–5321. [PubMed: 15100270]
23. Clark AG, Mackin KM, Foster MH. Tracking differential gene expression in MRL/MpJ versus C57BL/6 anergic B cells: Molecular markers of autiommunity. Biomarker Insights. 2008; 3:335–350. [PubMed: 19578517]
24. Foster MH, Fitzsimons MM. Lupus-like nephrotropic autoantibodies in nonautoimmune mice harboring an anti-laminin Ig heavy chain transgene. Molecular Immunology. 1998; 35:83–94. [PubMed: 9683254]
25. Clark AG, Mackin KM, Foster MH. Genetic elimination of alpha3(IV) collagen fails to rescue anti-collagen B cells. Immunology letters. 2011; 141(1):134–139. [PubMed: 21963654]
26. Oi V, Morrison SL, Herzenberg LA, Berg P. Immunglobulin gene expression in transformed lymphoid cells. Proc Natl Acad Sci USA. 1983; 80:825–829. [PubMed: 6402777]

27. Tybulewicz VLJ, Crawford CE, Jackson PK, Bronson RT, Mulligan RC. Neonatal Lethality and Lymphopenia in Mice with a Homozygous Disruption of the c-abl Proto-Oncogene. Cell. 1991; 65:1153–1163. [PubMed: 2065352]
28. Brochet X, Lefranc M-P, Giudicelli V. IMGT/V-Quest: the highly customized and integrated system for IG and TR standardized V-J and V-D-J sequence analysis. Nucleic Acids Res. 2008; 36:W503–W508. [PubMed: 18503082]
29. Foster MH, Cooperstone BG, Chen H. Anti-idiotypic monoclonal Ig specific for an anti-laminin Ig heavy chain transgene variable region. Hybridoma. 1998; 17(4):323–329. [PubMed: 9790066]
30. Amano H, Amano E, Moll T, Marinkovic D, Ibnou-Zekri N, Martinez-Soria E, et al. The Yaa mutation promoting murine lupus causes defective development of marginal zone B cells. J Immunol. 2003; 170(5):2293–2301. [PubMed: 12594250]
31. Moll T, Martinez-Soria E, Santiago-Raber M-L, Amano H, Pihlgren-Bosch M, Marinkovic D, et al. Differential Activation of Anti-Erythrocyte and Anti-DNA Autoreactive B Lymphocytes by the Yaa Mutation. J Immunol. 2005; 174:702–709. [PubMed: 15634889]
32. Pisitkun P, Deane JA, Difilippantonio MJ, Tarasenko T, Satterthwaite AB, Bolland S. Autoreactive B cell responses to RNA-related antigens due to TLR7 gene duplication. Science. 2006; 312(5780):1669–1672. [PubMed: 16709748]
33. Subramanian S, Tus K, Li QZ, Wang A, Tian XH, Zhou J, et al. A Tlr7 translocation accelerates systemic autoimmunity in murine lupus. Proc Natl Acad Sci U S A. 2006; 103(26):9970–9975. [PubMed: 16777955]
34. Santiago-Raber M-L, Kikuchi S, Borel P, Uematsu S, Akira S, Kotzin BL, et al. Evidence for Genes in Addition to Tlr7 in the Yaa Translocation Linked with Acceleration of Systemic Lupus Erythematosus. J Immunol. 2008; 181:1556–1562. [PubMed: 18606711]
35. Meffre E. The establishment of early B cell tolerance in humans: lessons from primary immunodeficiency diseases. Ann N Y Acad Sci. 2011; 1246(1):1–10. [PubMed: 22236425]
36. Isnardi I, Ng YS, Srdanovic I, Motaghedi R, Rudchenko S, von Bernuth H, et al. IRAK-4- and MyD88-dependent pathways are essential for the removal of developing autoreactive B cells in humans. Immunity. 2008; 29(5):746–757. [PubMed: 19006693]
37. Meyers G, Ng YS, Bannock JM, Lavoie A, Walter JE, Notarangelo LD, et al. Activation-induced cytidine deaminase (AID) is required for B-cell tolerance in humans. Proceedings of the National Academy of Sciences of the United States of America. 2011; 108(28):11554–11559. [PubMed: 21700883]
38. Kuraoka M, Holl TM, Liao D, Womble M, Cain DW, Reynolds AE, et al. Activation-induced cytidine deaminase mediates central tolerance in B cells. Proceedings of the National Academy of Sciences of the United States of America. 2011; 108(28):11560–11565. [PubMed: 21700885]
39. Menard L, Saadoun D, Isnardi I, Ng YS, Meyers G, Massad C, et al. The PTPN22 allele encoding an R620W variant interferes with the removal of developing autoreactive B cells in humans. The Journal of clinical investigation. 2011; 121(9):3635–3644. [PubMed: 21804190]
40. Murakami M, Tsubata T, Okamoto M, Shimizu A, Kumagai S, Imura H, et al. Antigen-induced apoptotic death of Ly-1 B cells responsible for autoimmune disease in transgenic mice. Nature. 1992; 357:77–80. [PubMed: 1574128]
41. Nisitani S, Sakiyama T, Honjo T. Involvement of IL-10 in induction of autoimmune hemolytic anemia in anti-erythrocyte Ig transgenic mice. Int Immunol. 1998; 10(8):1039–1047. [PubMed: 9723689]
42. Goodnow CC, Crosbie J, Adelstein S, Lavoie TB, Smith-Gill SJ, Brink RA, et al. Altered immunoglobulin expression and functional silencing of self-reactive B lymphocytes in transgenic mice. Nature. 1988; 334:676–682. [PubMed: 3261841]
43. Chang N-H, Cheung Y-H, Loh C, Pau E, Roy V, Cai Y-C, et al. B Cell Activating Factor (BAFF) and T Cells Cooperate to Breach B Cell Tolerance in Lupus-Prone New Zealand Black (NZB) Mice. PLoS One. 2010; 5(7):e11691. [PubMed: 20661465]
44. Santiago-Raber ML, Amano H, Amano E, Fossati-Jimack L, Swee LK, Rolink A, et al. Evidence that Yaa-induced loss of marginal zone B cells is a result of dendritic cell-mediated enhanced activation. Journal of autoimmunity. 2010; 34(4):349–355. [PubMed: 20149596]

45. Bendelac A, Bonneville M, Kearney JF. Autoreactivity by design: innate B and T lymphocytes. Nature reviews Immunology. 2001; 1(3):177–186.
46. Meyer-Bahlburg A, Rawlings DJ. Differential impact of Toll-like receptor signaling on distinct B cell subpopulations. Frontiers in bioscience : a journal and virtual library. 2012; 17:1499–1516. [PubMed: 22201817]
47. Grimaldi CM, Michael DJ, Diamond B. Cutting edge: expansion and activation of a population of autoreactive marginal zone B cells in a model of estrogen-induced lupus. J Immunol. 2001; 167(4):1886–1890. [PubMed: 11489967]
48. Mackay F, Woodcock SA, Lawton P, Ambrose C, Baetscher M, Schneider P, et al. Mice transgenic for BAFF develop lymphocytic disorders along with autoimmune manifestations. J Exp Med. 1999; 190(11):1697–1710. [PubMed: 10587360]
49. Liu Y, Li L, Kumar KR, Xie C, Lightfoot S, Zhou XJ, et al. Lupus susceptibility genes may breach tolerance to DNA by impairing receptor editing of nuclear antigen-reactive B cells. Journal of immunology. 2007; 179(2):1340–1352.
50. Duan B, Croker BP, Morel L. Lupus resistance is associated with marginal zone abnormalities in an NZM murine model. Laboratory investigation; a journal of technical methods and pathology. 2007; 87(1):14–28.
51. Duan B, Niu H, Xu Z, Sharpe AH, Croker BP, Sobel ES, et al. Intrafollicular location of marginal zone/CD1d(hi) B cells is associated with autoimmune pathology in a mouse model of lupus. Laboratory investigation; a journal of technical methods and pathology. 2008; 88(9):1008–1020.
52. Shao WH, Kuan AP, Wang C, Abraham V, Waldman MA, Vogelgesang A, et al. Disrupted Mer receptor tyrosine kinase expression leads to enhanced MZ B-cell responses. Journal of autoimmunity. 2010; 35(4):368–374. [PubMed: 20822883]
53. Zhou Z, Niu H, Zheng YY, Morel L. Autoreactive marginal zone B cells enter the follicles and interact with CD4+ T cells in lupus-prone mice. BMC immunology. 2011; 12:7. [PubMed: 21251257]
54. Wither JE, Loh C, Lajoie G, Heinrichs S, Cai YC, Bonventi G, et al. Colocalization of expansion of the splenic marginal zone population with abnormal B cell activation and autoantibody production in B6 mice with an introgressed New Zealand Black chromosome 13 interval. Journal of immunology. 2005; 175(7):4309–4319.
55. Foster MH, Zhang Y, Clark AG. Deconstructing B cell tolerance to basement membranes. Arch Immunol Ther Exp. 2006; 54:1–11.
56. Al-Qahtani A, Xu Z, Zan H, Walsh CM, Casali P. A role for DRAK2 in the germinal center reaction and the antibody response. Autoimmunity. 2008; 41(5):341–352. [PubMed: 18568639]
57. Wellmann U, Letz M, Schneider A, Amann K, Winkler TH. An Ig mu-heavy chain transgene inhibits systemic lupus erythematosus immunopathology in autoimmune (NZB × NZW)F1 mice. Int Immunol. 2001; 13(12):1461–1469. [PubMed: 11717187]
58. Jacob N, Stohl W. Autoantibody-dependent and autoantibody-independent roles for B cells in systemic lupus erythematosus: past, present, and future. Autoimmunity. 2010; 43(1):84–97. [PubMed: 20014977]
59. Roark JH, Kuntz CL, Nguyen K, Caton AJ, Erikson J. Breakdown of B cell tolerance in a mouse model of systemic lupus erythematosus. J Exp Med. 1995; 181:1157–1167. [PubMed: 7532679]
60. Rubio CF, Kench J, Russell DM, Yawger R, Nemazee D. Analysis of central B cell tolerance in autoimmune-prone MRL/lpr mice bearing autoantibody transgenes. J Immunol. 1996; 157:65–71. [PubMed: 8683157]
61. Santulli-Marotto S, Qian Y, Ferguson S, Clarke SH. Anti-Sm B Cell Differentiation in Ig Transgenic MRL/Mp-lpr/lpr Mice: Altered Differentiation and an Accelerated Response. J Immunol. 2001; 166(8):5292–5299. [PubMed: 11290816]
62. Chen C, Li H, Tian Q, Beardall M, Xu Y, Casanova N, et al. Selection of anti-double-stranded DNA B cells in autoimmune MRL-lpr/lpr mice. J Immunol. 2006; 176(9):5183–5190. PubMed PMID: 16621982. [PubMed: 16621982]
63. Friedmann D, Yachimovich N, Mostoslavsky G, Pewzner-Jung Y, Ben-Yehuda A, Rajewsky K, et al. Production of high affinity autoantibodies in autoimmune New Zealand Black/New Zealand

white F1 mice targeted with an anti-DNA heavy chain. J Immunol. 1999; 162:4406–4416. [PubMed: 10201976]

64. Wellmann U, Werner A, Winkler TH. Altered selection processes of B lymphocytes in autoimmune NZB/W mice, despite intact central tolerance against DNA. Eur J Immunol. 2001; 31:2800–2810. [PubMed: 11536179]
65. Spatz L, Saenko V, Iliev A, Jones L, Geskin L, Diamond B. Light chain usage in anti-double-stranded DNA B cell subsets: Role in cell fate determination. J Exp Med. 1997; 185:1317–1326. [PubMed: 9104818]
66. Steeves MA, Marion TN. Tolerance to DNA in (NZB × NZW)F1 mice that inherit an anti-DNA V(H) as a conventional micro H chain transgene but not as a V(H) knock-in transgene. J Immunol. 2004; 172(11):6568–6577. [PubMed: 15153471]
67. Duong BH, Ota T, Ait-Azzouzene D, Aoki-Ota M, Vela JL, Huber C, et al. Peripheral B cell tolerance and function in transgenic mice expressing an IgD superantigen. Journal of immunology. 2010; 184(8):4143–4158.
68. Roes J, Rajewsky K. Immunoglobulin D (IgD)-deficient mice reveal an auxiliary receptor function for IgD in antigen-mediated recruitment of B cells. The Journal of experimental medicine. 1993; 177(1):45–55. [PubMed: 8418208]
69. Nitschke L, Kosco MH, Kohler G, Lamers MC. Immunoglobulin D-deficient mice can mount normal immune responses to thymus-independent and -dependent antigens. Proceedings of the National Academy of Sciences of the United States of America. 1993; 90(5):1887–1891. [PubMed: 8446604]
70. Woodward EJ, Thomas JW. Multiple germline kappa light chains generate anti-insulin B cells in nonobese diabetic mice. Journal of immunology. 2005; 175(2):1073–1079.
71. Henry RA, Kendall PL, Woodward EJ, Hulbert C, Thomas JW. Vkappa polymorphisms in NOD mice are spread throughout the entire immunoglobulin kappa locus and are shared by other autoimmune strains. Immunogenetics. 2010; 62(8):507–520. [PubMed: 20556377]
72. Trepicchio W Jr, Barrett KJ. The Igh-V locus of MRL mice: Restriction fragment length polymorphism in eleven strains of mice as determined with VH and D gene probes. J Immunol. 1985; 134:2734–2739. [PubMed: 2982952]
73. Kompfner E, Oliveira P, Montalbano A, Feeney AJ. Unusual germline DSP2 gene accounts for all apparent V-D-D-J rearrangements in newborn, but not adult, MRL mice. Journal of immunology. 2001; 167(12):6933–6938.

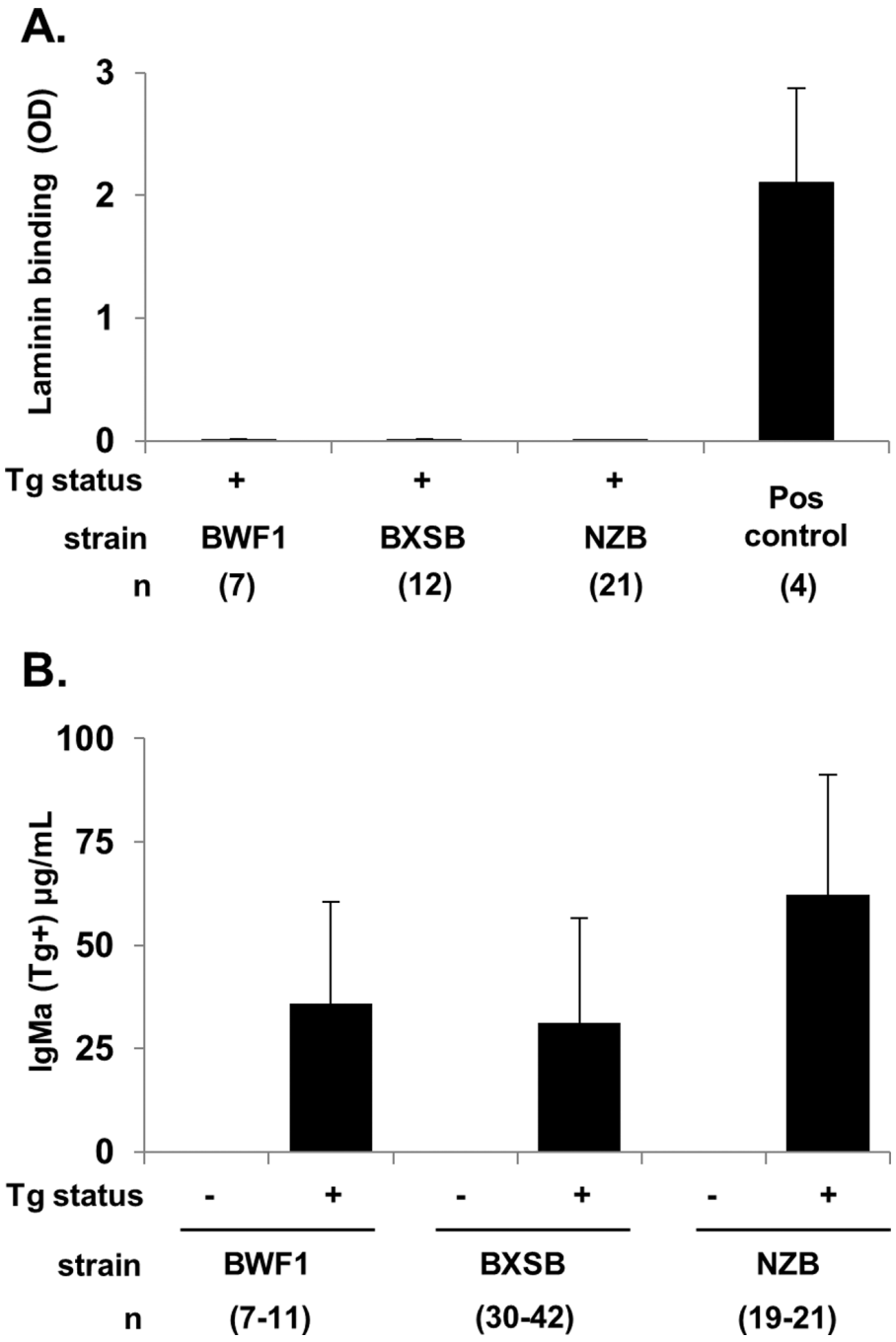

Figure 1.

Serum transgene-encoded Ig in BWF1, BXSB, and NZB lupus mice. A) Laminin binding: OD_{405} on antigen coated wells minus the OD_{405} on diluent-only coated wells, based on duplicate serum samples. The positive control is anti-laminin supernatant A10C. Only Tg+ mice are shown. B) IgMa (transgenic Ig) concentration for Tg+ relative to non-transgenic subjects for each strain. Results are expressed as the mean ± SD; all Tg+ to non-Tg comparisons within the same strain are $p<0.05$. Number of subjects, from 5-12 independent experiments per strain, is shown in parenthesis.

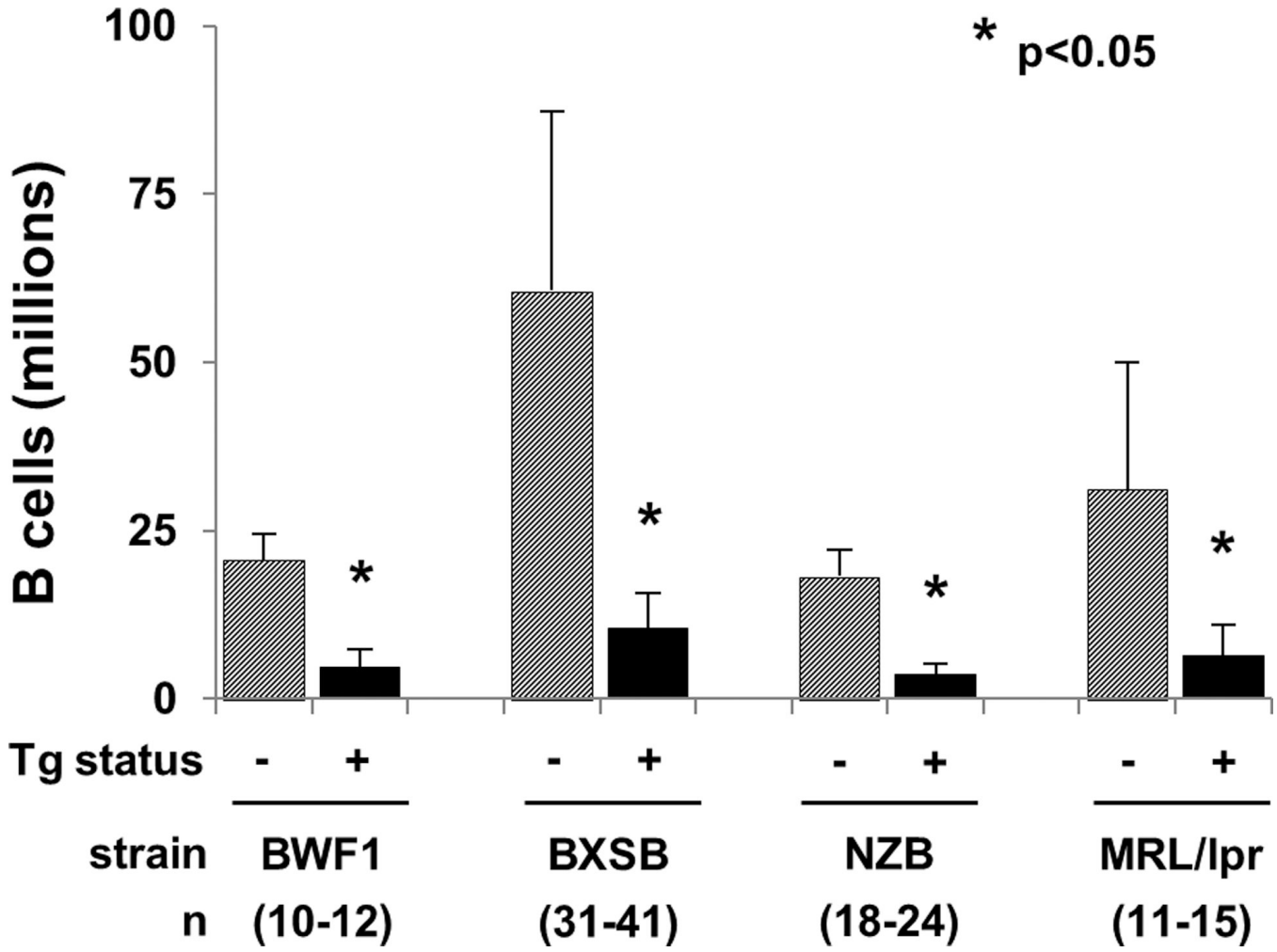

Figure 2.

Splenic B cell counts in lupus mice bearing the anti-laminin Ig transgene, and nontransgenic controls, in millions. Mean ± SD; *p<0.05 for Tg+ versus non-Tg subjects from the same strain. Number of subjects, from 5-11 independent experiments per strain, is denoted in parenthesis.

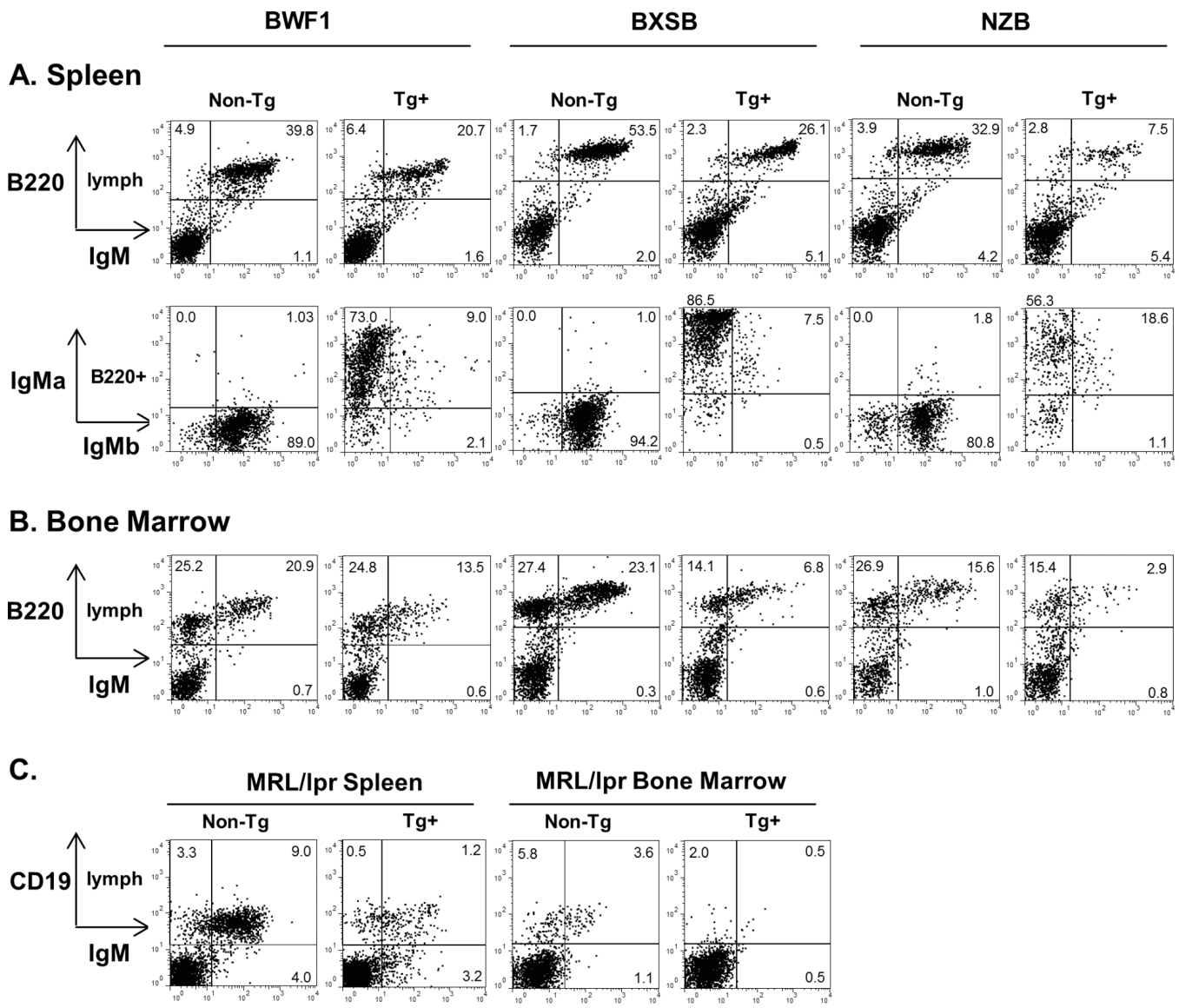

Figure 3.

Representative surface FACS plots for lupus mice bearing the anti-laminin Ig transgene. Lymphocytes were gated based on FSC and SSC properties, with additional gating as indicated. A) Splenocytes, and B) Bone marrow for the BWF1, BXSB, and NZB backgrounds. B220 is a B cell marker. IgMa = transgenic heavy chain, IgMb = endogenous heavy chain. C) Splenocytes and bone marrow for the MRL/lpr background. CD19 is a B cell marker; the presence of abnormal B220+ T cells in MRL/lpr precludes use of B220 in this strain. Tg+ = LamH transgenic, non-Tg = nontransgenic.

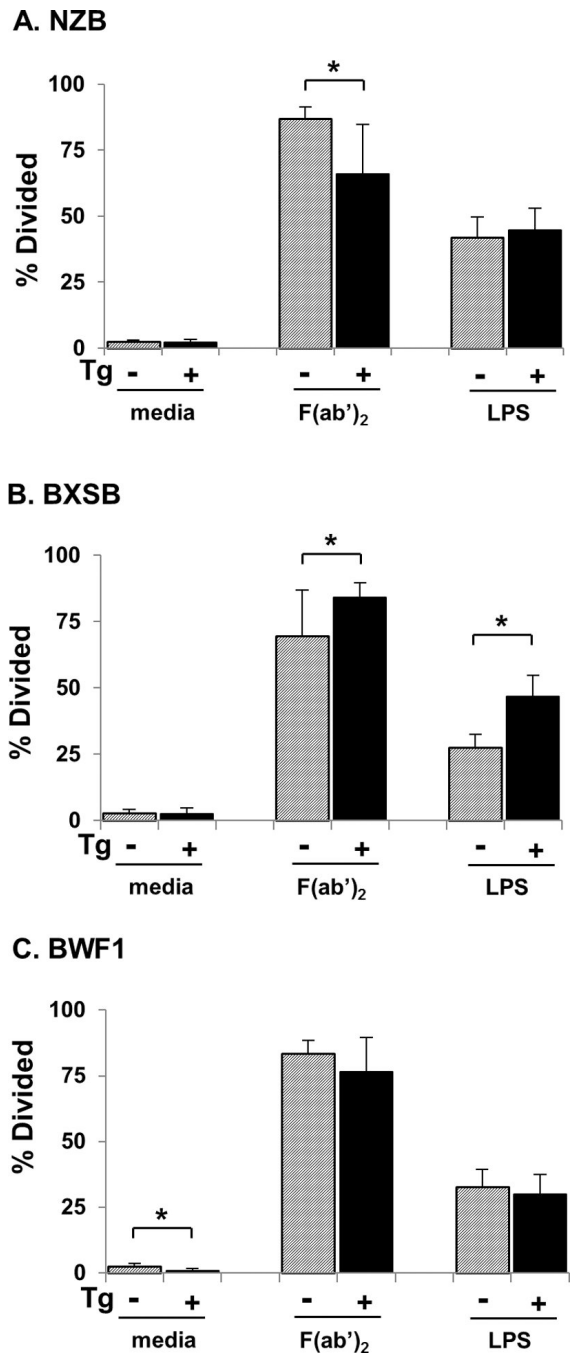

Figure 4.

Proliferation of residual B cells in Tg+ lupus mice. B cells purified by CD43 negative selection were cultured in media alone, stimulated with LPS, or subjected to B cell receptor crosslinking using anti-IgM F(ab')$_2$ as indicated. Shown is the percentage of cells that underwent division during 2.5 days of culture, mean ± SD. *$p<0.05$ for Tg+ vs non-Tg in the same strain with the same stimulant.

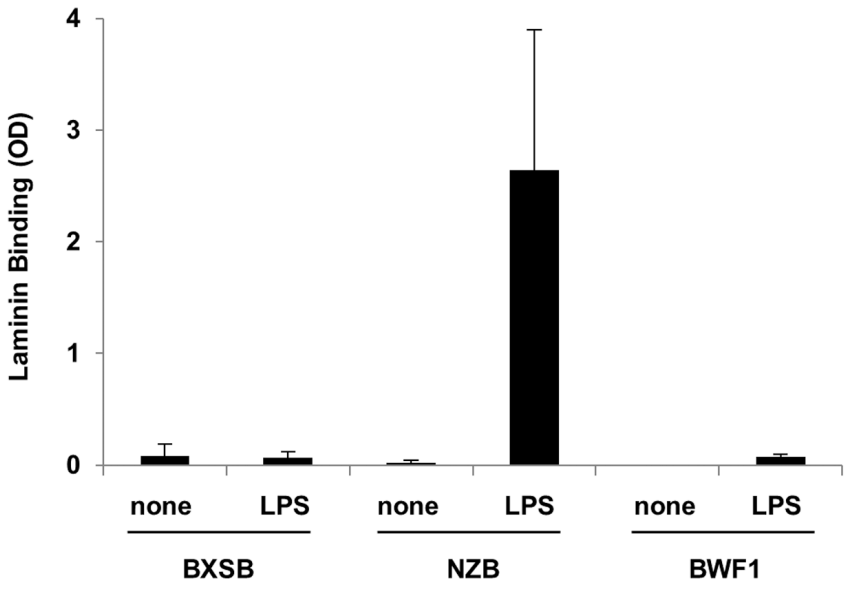

Figure 5.

B cell autoantibody secretion. Purified B cells were incubated with medium alone (“none”) or with medium containing LPS for 8-10 days prior to assay of supernatant by ELISA for anti-laminin IgMa. Shown is the mean ± SD for OD_{405} for binding of undiluted supernatant to laminin coated wells minus binding to wells coated with diluent only. Positive control anti-laminin IgG H50-9 value was 1.59 ± 0.13, and anti-laminin IgMa A10C supernatant was 1.62 ± 0.12.

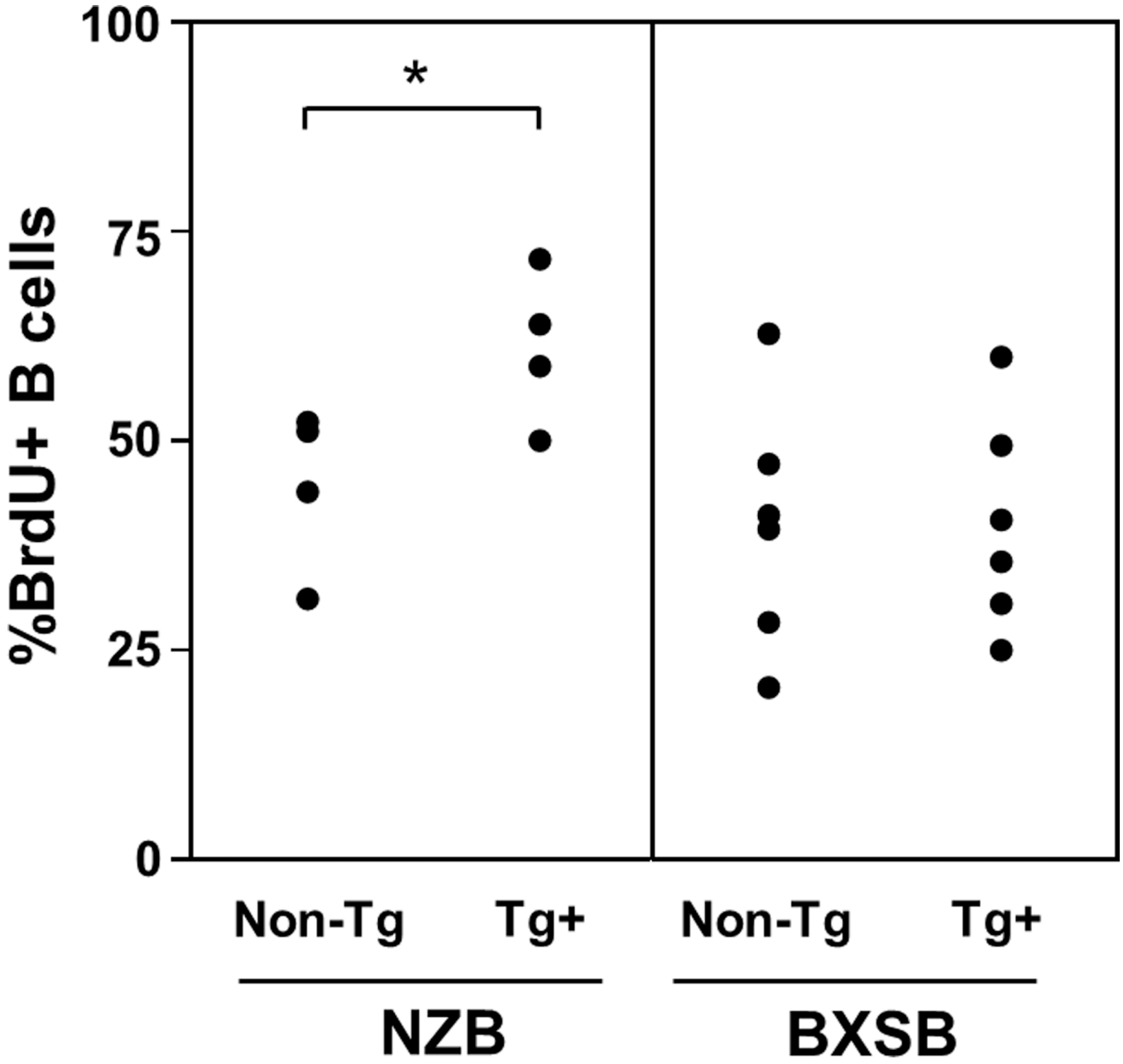

Figure 6.
Percentage of splenic B cells positive for BrdU incorporation, following 30 days of in vivo exposure, for Tg+ NZB and BXSB subjects and nontransgenic littermate controls.

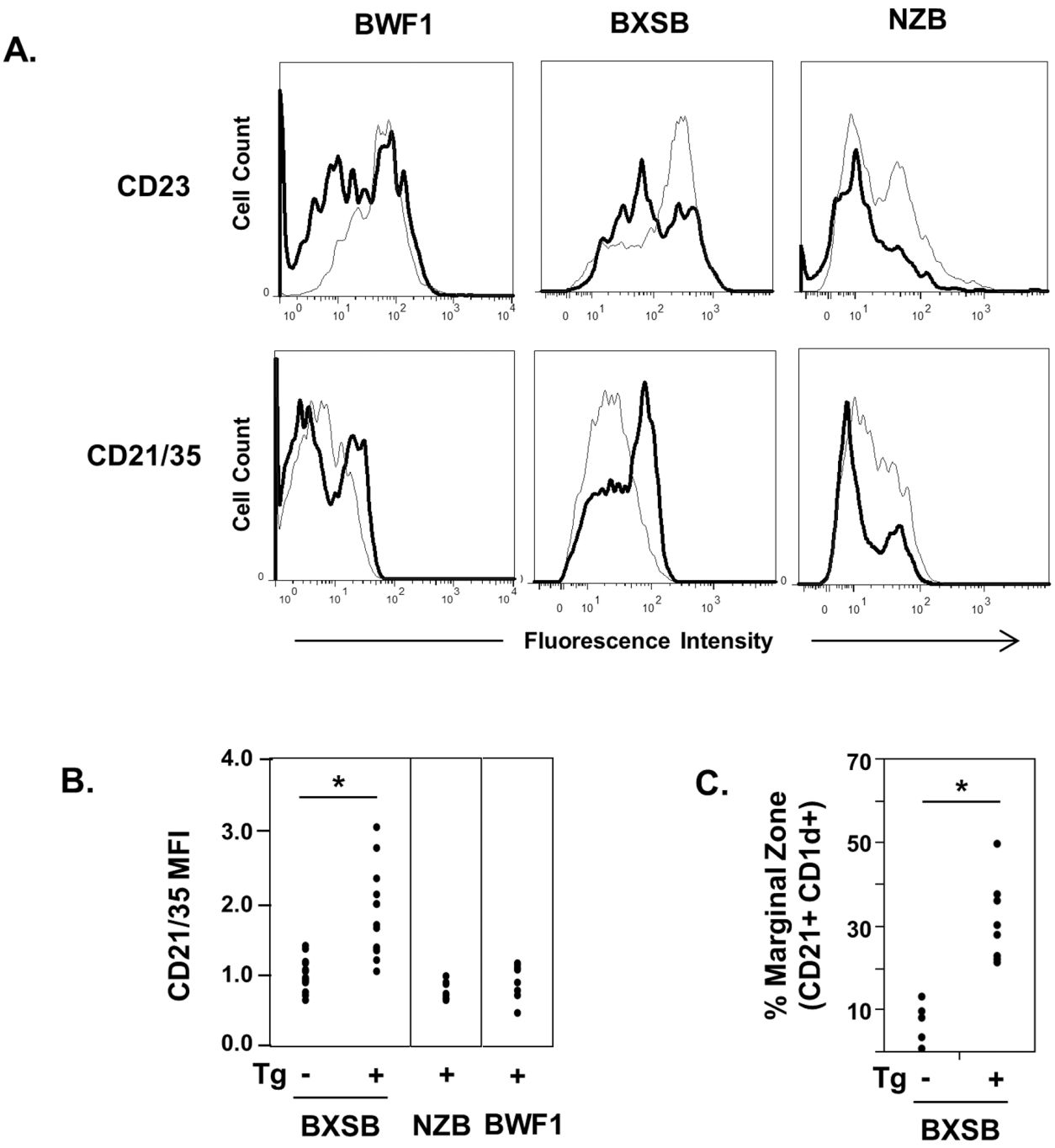

Figure 7.

Splenic B cell expression of CD23 and CD21/35 and marginal zone markers. A) Representative fluorescence intensity histograms of CD23-PE or CD21/35-FITC on B220+ gated B cells from LamH Ig transgenic lupus mice (bold line) relative to B cells from non-Tg controls of the same strain (light grey line). B) Scatterplot of normalized mean fluorescence intensity of CD21/35 on BXSB, NZB, and BWF1 Tg+ B cells. Fluorescence was normalized in each experiment to the mean fluorescence of non-Tg subjects for each strain, shown for BXSB. C) Scatterplot of the percentage of B220+ cells identified as marginal zone cells by the CD21+ CD1d+ marker combination in LamH Ig Tg mice and non-Tg controls. BXSB mice used for marginal zone analysis were 14-15.5 months of age,

excepting two non-Tg BXSB males who were 4.5 and 5.5 months of age. *p<0.05 vs non-Tg.

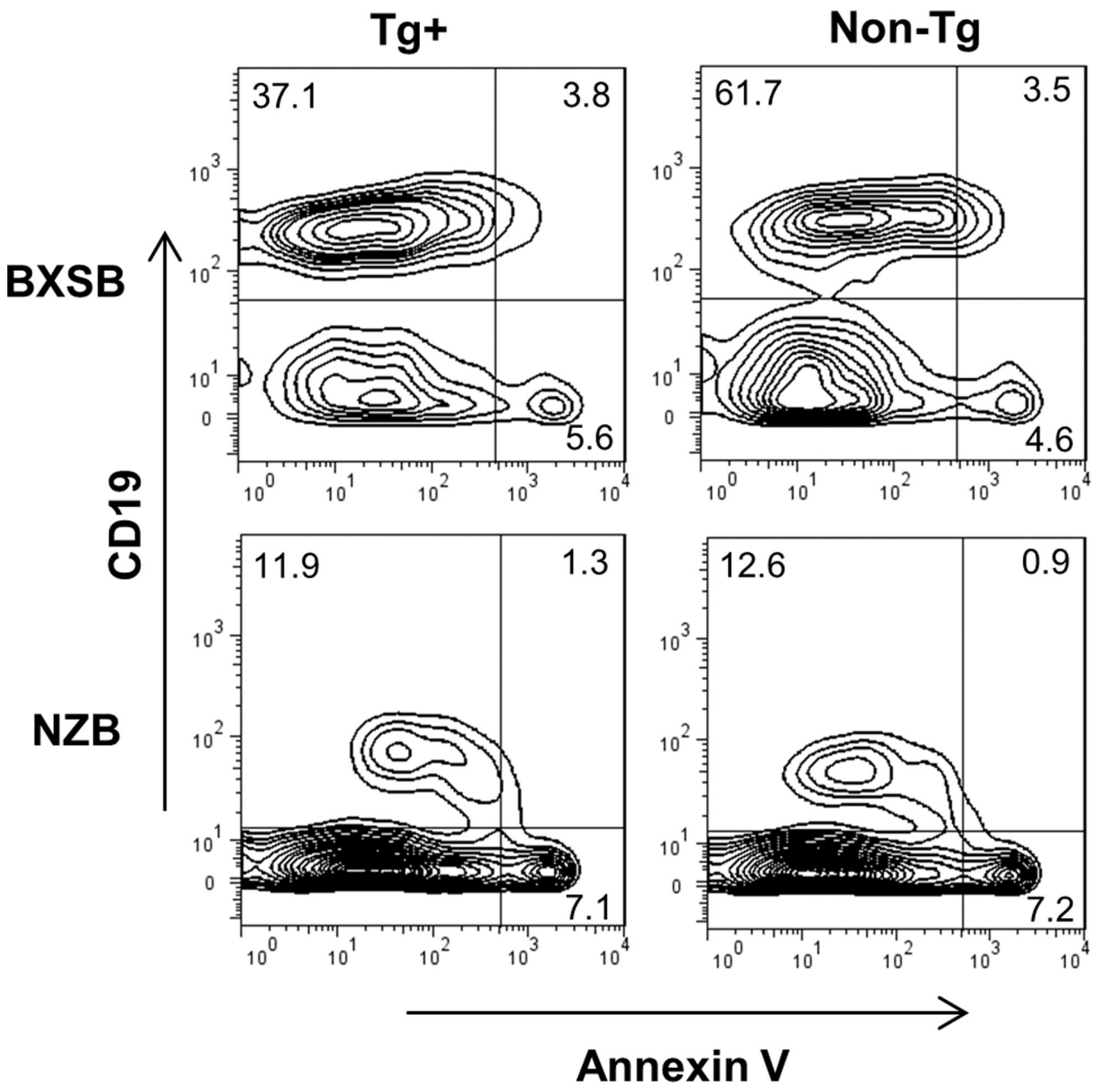

Figure 8.

Apoptosis in BXSB and NZB splenic lymphocytes. RBC-depleted splenocytes were stained with annexin V, 7-AAD, and CD19 and flow cytometric data acquired within 30 minutes of staining. Shown are representative plots gated initially on lymphocytes by light scatter properties. The % of lymphocytes are indicated in the plots; the percent annexin+ of B cells in these representative plots are 9.3% Tg+ and 5.4% non-Tg for the BXSB, and 9.8% Tg+ and 6.7% non-Tg for the NZB.

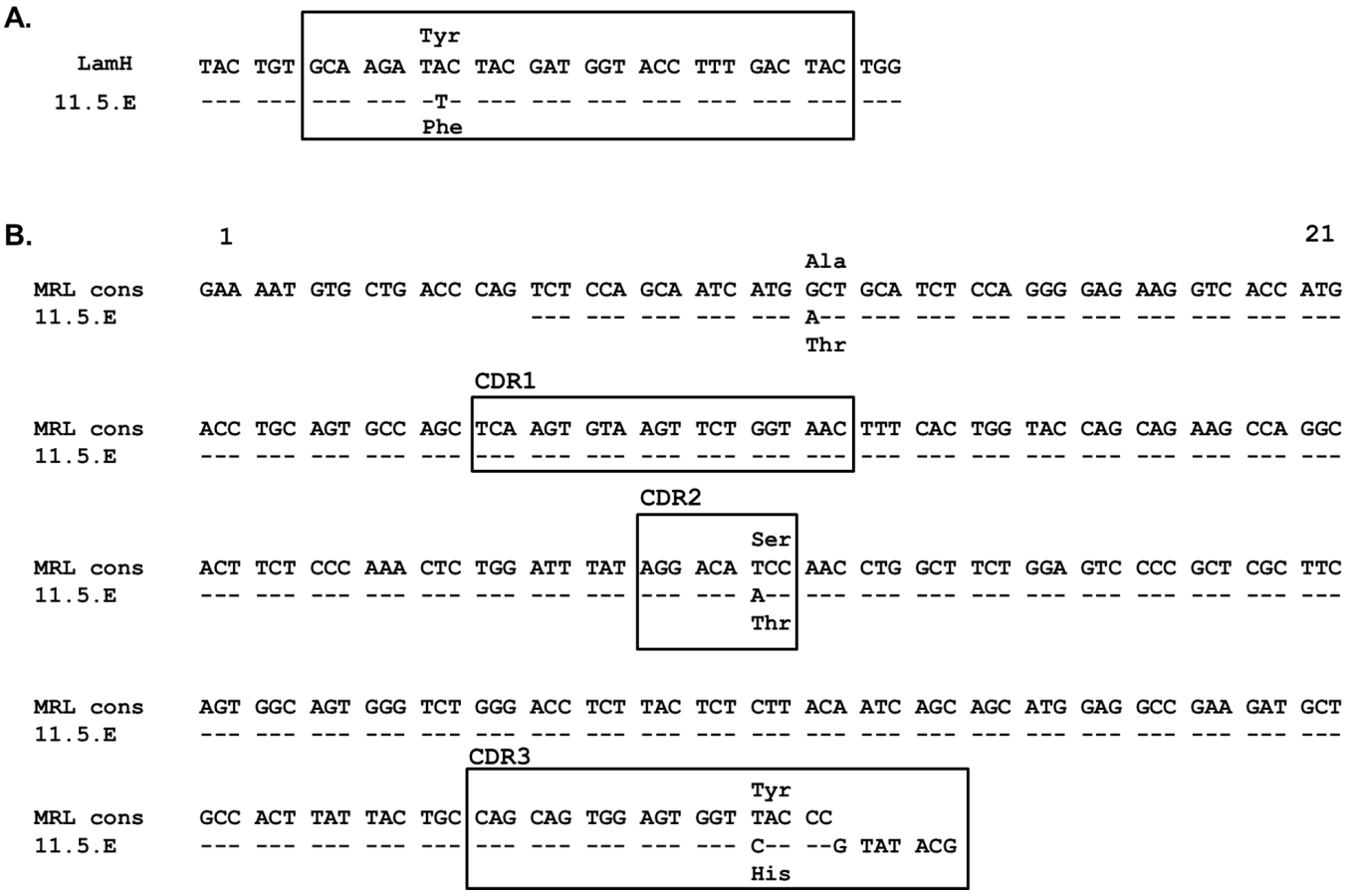

Figure 9.

Sequence analysis of Tg+ MRL/lpr laminin-binding hybridoma 11.5.E. A) Comparison of the LamH transgene and 11.5.E hybridoma H chain CDR3 sequences (boxed). B) Comparison of an MRL-derived IGKV4 consensus sequence and the light chain V region sequence of hybridoma 11.5.E. The consensus MRL sequence was compiled from MRL +/+ and MRL/lpr IGKV4-encoded Ig identified in GenBank with accession numbers: M18239, M18237.1, M18238, M18236, M22451, U51464, U51459, D14630, U28349, L09009, and U26476. CDRs and codons are delineated according to the IMGT numbering system in IMGT/V-QUEST [27]. The 11.5.E sequences have been submitted to GenBank under accession number JQ513389.

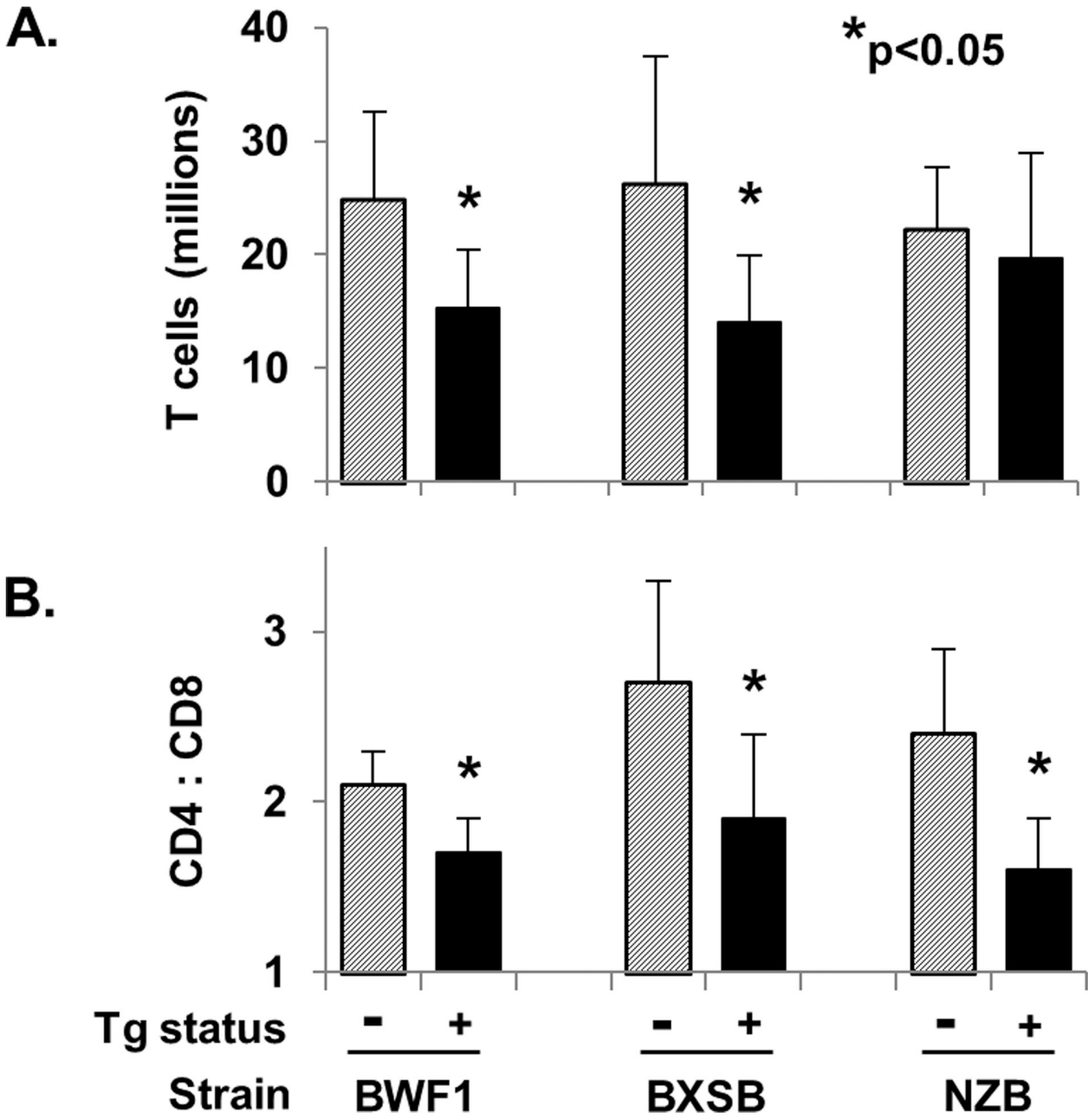

Figure 10.
T cell counts and CD4:CD8 ratios. Total T cell count was calculated as total splenocytes × %lymphocytes × %CD3+. *p<0.05 versus non-Tg mice of the same strain.

Table 1

B cell profiles of LamH Tg+ and Non-Tg spleen (A) and Bone marrow (B) by lupus strain [a]

	BWF1		BXSB		NZB		MRL/lpr	
	Non-Tg	**Tg+**	**Non-Tg**	**Tg+**	**Non-Tg**	**Tg+**	**Non-Tg**	**Tg+**
A. Spleen								
B cells (millions)	23.2 ± 6.1 (13)	5.4 ± 2.9* (15)	60.6 ± 26.7 (31)	10.6 ± 5.3* (41)	18.2 ± 4.0 (18)	3.6 ± 1.6* (24)	31.2± 18.9 (11)	6.4 ± 4.7* (15)
% B cell decrease (vs Non-Tg)	-	76.7	-	82.5	-	80.2	-	75.6
%IgMa+	3.3 ± 3.1 (13)	82.6 ± 8.9* (15)	1.7 ± 1.8 (30)	86.7 ± 6.5* (41)	1.9 ± 1.3 (18)	61.1 ± 11.5* (24)		
%IgMb+	84.3 ± 7.9 (13)	15.8 ± 6.9* (15)	82.6 ± 8.3 (30)	12.9 ± 4.9* (41)	80.9 ± 7.2 (18)	24.4 ± 12.7* (24)		
%Lambda+	3.2 ± 1.1 (13)	2.0 ± 1.0* (15)	3.7 ± 1.5 (19)	7.1 ± 2.5* (26)	5.5 ± 1.8 (11)	8.9 ± 4.3* (14)	11.6± 9.1 (7)	6.9 ± 3.8 (7)
Surface Ig MFI	1.0 ± 0.2 (13)	0.6 ± 0.3* (15)	1.0 ± 0.1 (19)	1.0 ± 0.1 (21)	1.0 ± 0.1 (13)	0.6 ± 0.1* (16)	1.0 ± 0.1 (7)	0.4 ± 0.2* (7)
B. Bone Marrow								
% B cells Of lymph	42.9 ± 11.7 (13)	35.1 ± 15.4 (15)	45.6 ± 13.1 (23)	27.5 ± 10.7* (27)	32.8 ± 13.3 (18)	23.4 ± 10.3* (24)	10.8 ± 5.4 (5)	3.7 ± 1.9 (5)
%IgM+ of B cells	44.0 ± 7.5 (13)	30.3 ± 6.1* (15)	51.5 ± 16.9 (26)	34.6 ± 7.5* (34)	47.6 ± 16.1 (17)	33.3 ± 20.2* (20)	37.8 ± 14.7 (5)	27.8 ± 7.2 (5)

[a] Data expressed as mean ± SD; number of subjects is shown in parenthesis. Average age of subjects included in this table, in months: BWF1 non-Tg: 3.4 ± 1.5, Tg+: 3.7 ± 1.3; BXSB non-Tg: 4.6 ± 2.3, Tg +: 5.1 ± 2.2; NZB non-Tg: 3.9 ± 2.0, Tg+ 4.5 ± 2.3; MRL/lpr non-Tg: 4.6 ± 1.8, Tg+ 4.4 ± 1.5.

* $p<0.05$ versus non-Tg of the same strain.

Table 2

B cell surface expression of activation and development markers[a]

	BWF1		BXSB		NZB	
	Non-Tg	**Tg+**	**Non-Tg**	**Tg+**	**Non-Tg**	**Tg+**
CD 5	1.0 ± 0.1 (8)	1.4 ± 0.2* (9)	1.0 ± 0.2 (14)	1.7 ± 0.9* (16)	1.0 ± 0.1 (8)	1.6 ± 0.3* (8)
CD23	1.0 ± 0.1 (8)	0.8 ± 0.2 (9)	1.0 ± 0.2 (14)	0.9 ± 0.1* (16)	1.0 ± 0.1 (13)	0.6 ± 0.1* (16)
CD86	1.0 ± 0.1 (5)	0.8 ± 0.1* (6)	1.0 ± 0.4 (13)	1.0 ± 0.4 (16)	1.0 ± 0.1 (8)	1.3 ± 0.2* (8)
%CD21/35	61.0 ± 6.1 (7)	49.0 ± 13.0* (8)	57.1 ± 15.6 (13)	68.8 ± 9.0* (18)	61.4 ± 9.6 (8)	39.2 ± 7.4* (8)

[a]Expressed as the linear mean fluorescence intensity of the marker in B220+ gated cells normalized to the expression of non-Tg mice of the same strain, or for CD21/35 as a percentage of total B220+ cells expressing the marker. Mean ± SD is shown, with the number of subjects in parenthesis below.

*$p<0.05$ for Tg+ vs Non-Tg in same strain. One outlier from the BXSB non-Tg group, with a normalized CD86 MFI of 4.8, was omitted from this analysis.